nature medicine

Article

https://doi.org/10.1038/s41591-024-03449-x

Donor-derived GD2-specific CAR T cells in relapsed or refractory neuroblastoma

Received: 9 February 2024

Accepted: 4 December 2024

Published online: 15 January 2025

Check for updates

A list of authors and their affiliations appears at the end of the paper

Allogeneic chimeric antigen receptor (CAR) T cells targeting disialoganglioside-GD2 (ALLO_GD2-CART01) could be a therapeutic option for patients with relapsed or refractory, high-risk neuroblastoma (r/r HR-NB) whose tumors did not respond to autologous GD2-CART01 or who have profound lymphopenia. We present a case series of five children with HR-NB refractory to more than three different lines of therapy who received ALLO_GD2-CART01 in a hospital exemption setting. Four of them had previously received allogeneic hematopoietic stem cell transplantation. All patients experienced grade 2 or 3 cytokine release syndrome and one grade 2 neurotoxicity. Moderate acute graft-versus-host-disease occurred in four patients. ALLO_GD2-CART01 persisted for >6 weeks. Post-treatment, two complete responses were achieved and one maintained; in addition, one partial response and one stable disease were observed. Comparing the transcriptomic profiles obtained by RNA sequencing analyses of drug products with patient-matched, peripheral blood ALLO_GD2-CART01 collected at expansion, we found upregulation of genes associated with T cell activation and migration. In addition, after infusion, transcriptomic signaling analysis showed enrichment of genes involved in response to decreased oxygen levels, humoral immune response, cell polarization and immune-synapse formation. In comparison to autologous CAR T cells, ALLO_GD2-CAR T cells were characterized by pathways associated with T cell proliferation, immune-synapse formation and cell chemotaxis. The safety and efficacy of ALLO_GD2-CART01 in children with r/r HR-NB deserve further investigation in a prospective trial.

Despite the intensive, multimodal treatment, including an intensified induction chemotherapy, surgery, high-dose (HD) chemotherapy with autologous hematopoietic stem cell (HSC) rescue, radiotherapy and maintenance therapy with the differentiating agent 13-*cis*-retinoic acid (CRA) and the monoclonal antibody directed against the disialoganglioside GD2, 50–60% of patients with high-risk neuroblastoma (HR-NB) experience a poor tumor response or relapse, with poor chances of then being rescued[1,2]. Relapsed or refractory (r/r) HR-NB is associated with a dismal outcome, because long-term, disease-free survival does not exceed 10–15%[3].

We recently reported the interim results of our phase I/II clinical trial (NCT03373097) showing that autologous T cells genetically modified to express a third-generation (CD28-4.1BB) chimeric antigen receptor (CAR) targeting GD2 (GD2-CART01) represent a valuable option for patients with r/r HR-NB[4]. In particular, we showed that the patients with a lower disease burden at the time of infusion have a remarkable 3-year, event-free survival approaching 60% when treated with GD2-CAR T cells. The achievement of a low tumor burden may require the use of HD chemotherapy or *meta*-iodobenzylguanidine (MIBG) therapy that cannot be administered in patients who fail to collect autologous

e-mail: franco.locatelli@opbg.net

CD34$^+$ cells. Moreover, a proportion of patients do not have access to autologous CAR T cells as a result of a profound lymphopenia, preventing the collection of an adequate number of T cells. In addition, various intrinsic factors related to T cells, including the fitness of harvested T cells, the manufacturing process, prior treatment regimens and the phenotype of infused T cells, have been shown to correlate with clinical outcomes in patients receiving CAR T cell products[5].

To improve the manufacturing success, T cell fitness and overall drug product quality, we explored the use of allogeneic GD2-CAR T cells (ALLO_GD2-CART01), generated from either a fully human leukocyte antigen (HLA)-matched or an haploidentical donor, employing the same third-generation construct previously tested in the clinical trial using autologous (AUTO) GD2-CART01 (ref. 4). The presence of the inducible caspase 9 (iC9) suicide gene in the construct increases the safety profile of the approach, enabling the prompt elimination of proliferating CAR$^+$ cells on occurrence of severe toxicity. ALLO_GD2-CART01 was used in patients with advanced disease, who had no alternative therapeutic options available and one or both of the following: (1) profound lymphopenia preventing collection of autologous T cells and (2) a disease that had failed a previous treatment with autologous GD2-CART01.

In this case series, we reported the results of five patients with NB refractory to multiple, heterogeneous lines of prior treatment, who received ALLO_GD2-CART01 in a hospital exemption (HE) setting, after having exhausted any alternative, potentially curative, treatment. All treatments were previously approved by both the competent ethical committee and the national competent authority.

To gain more insights on the use of ALLO_GD2-CART01, we performed RNA sequencing (RNA-seq) studies to characterize the transcriptional signature of both CAR T cells present in the drug product and collected from peripheral blood (PB) at different time points after infusion.

Results

Patients' characteristics

Between February 2022 and January 2024, we treated five patients who had r/r HR-NB with ALLO_GD2-CART01 in an HE setting (a swimmer plot, summarizing both the previous history and the outcome after ALLO_GD2-CART01, is shown in Fig. 1a; patient characteristics and previous lines of treatment, heterogeneous and different across patients, are summarized in Table 1). All patients had tumors that had not responded to more than three lines of therapy, including autologous GD2-CART01 for two of them. The reasons for proceeding to ALLO_GD2-CART01 were lack of alternative, potentially curative therapeutic options and (1) severe lymphopenia (patient 1 (Pt1), Pt4 and Pt5) and (2) failure of previous AUTO_GD2-CART01 (Pt2 and Pt3). Importantly, all patients who were candidates to receive ALLO_GD2-CART01 were successfully treated, with no drop-out from the planned approach.

All these five patients also received allogeneic hematopoietic stem cell transplantation (HSCT) either before (Pt1, -3, -4 and -5) or after (Pt2) ALLO_GD2-CART01. The reasons for the previous allogeneic HSCT were: (1) indications for HD chemotherapy or [^{131}I]MIBG and failure to collect autologous CD34$^+$ cells (Pt1, -3 and -5); (2) consolidation of a complete remission (CR), in combination with dinutuximab-β (DB), as per clinical trial active in Germany (NCT02258815) (Pt4); and (3) prolonged, severe cytopenia (Pt2).

Data on patient follow-up were reported as of 30 June 2024.

Donor and HSCT characteristics and outcome

The characteristics of the donors of T cells and HSCs are detailed in Table 1. Briefly, Pt1 received haploidentical HSCs from the mother, after a conditioning regimen based on HD-[^{131}I]MIBG and melphalan. The disease status before HSCT was progressive disease (PD). Pt2 was transplanted, in CR, from a fully HLA-matched sibling, after having received ALLO_GD2-CART01, and received cyclophosphamide (50 mg kg^{-1} d^{-1} for 4 d) alone as conditioning therapy, because of profound and prolonged cytopenia. Pt3 received a haploidentical transplantation from the father, in stable disease (SD), and the conditioning regimen was based on the combination of busulfan, thiotepa and melphalan. Pt4 received a haploidentical rescue from the mother after HD-[^{131}I]MIBG therapy without any relevant toxicity. Pt5 received, in CR, a haploidentical transplantation from the mother, after a conditioning regimen based on busulfan, thiotepa and melphalan. In all patients, complete donor chimerism was confirmed by short tandem repeat analysis in the PB.

ALLO_GD2-CART01 manufacturing and characteristics of the drug products

ALLO_GD2-CART01 was successfully manufactured for all five patients using the same manufacturing process already applied for the production of AUTO_GD2-CART01. The median T cell number at the end of production of the ALLO_GD2-CART01 was 3.85×10^9 (range 2.4×10^9– 4.76×10^9), with a median transduction efficiency and cell viability, respectively, of 70.1% (range 62.8–76.5%) and 94.4% (range 88.5–96.7%).

Drug products were also characterized for the percentage of CD3$^+$ cells, CD4 and CD8 subsets, as well as the memory profile (Fig. 2a,b). In particular, the ALLO_GD2-CART01 drug product is characterized by a large predominance of CD4$^+$ or CD8$^+$ central memory CAR$^+$ T cells (in three of five; Fig. 2b), with a significant lower percentage of naive CD4$^+$CAR$^+$ T cells and naive and terminal differentiated effector memory (TEMRA) CD8$^+$CAR$^+$ T cells compared with the AUTO_GD2-CART01 drug products for the children enrolled in the clinical trial[4] NCT03373097 (Extended Data Fig. 1).

Patients' outcome after ALLO_GD2-CART01

ALLO_GD2-CART01 was infused on day + 62 after allogeneic HSCT in Pt1, day + 72 in Pt3, day + 73 in Pt4 and 2.5 years after HSCT in Pt5, whereas Pt2 received the genetically engineered T cells generated from the HLA-identical sibling 89 d before allogeneic HSCT (with allo-HSCT

Fig. 1 | Background treatment and clinical outcomes of patients with r/r NB treated with ALLO-GD2-CAR T cell therapy. a, Swimmer plot of the five patients treated, including the treatment history before ALLO_GD2-CART01 in the years before infusion and the history after ALLO_GD2-CART01. Patients received the treatment according to HR-NBL1/SIOPEN (induction chemotherapy/HD-chemotherapy + auto-HSCT/surgery/radiotherapy/maintenance with dinutuximab-β + CRA) after either enrollment into the clinical trial or the same recommendations, outside the clinical trial (Pt1). **b**, ALLO_GD2-CART01 activity. Change in SIOPEN skeletal score at 6 weeks after infusion versus before infusion (left) in four of the five patients with skeletal disease before infusion of ALLO_GD2-CART01 (in Pt5 no skeletal disease was present before infusion of ALLO_GD2-CAR and, therefore, was not included). Right, upper, merged single-photon emission computed tomography and MIBG uptake scans showing a metastatic vertebral lesion from Pt2 at the indicated time points. Right, lower, MIBG scan of Pt4 showing the disseminated skeletal disease pre-infusion and the complete response observed 6 weeks after infusion. **c**, Details of the SIOPEN score at the different time points of treatment (that is, baseline, before allogeneic HSCT, before ALLO_GD2-CART01 and 6 weeks after ALLO_GD2-CART01). The baseline assessment for Pt5 is not applicable (NA) because it was performed at another center, 2.5 years previously with ALLO_GD2-CART01. [a]In Pt2, HSCT was administered after ALLO_GD2-CART01, therefore this time point coincides with 'After ALLO_GD2-CART01'. **d**, Toxicity profile of patients receiving ALLO_GD2-CART01 according to Lee's criteria and the ASTCT Consensus Grading for ICANS. AST:ALT, aspartate transaminase:alanine transaminase. [a]Requires activation of the iC9; [b]GvHD was treated with intravenous administration of steroids (1 mg per kg per d, for 1 d in Pt1, 11 d and subsequently tapered in Pt2, 15 d and subsequently tapered in Pt3 and 2 d in Pt4).

https://doi.org/10.1038/s41591-024-03449-x

a

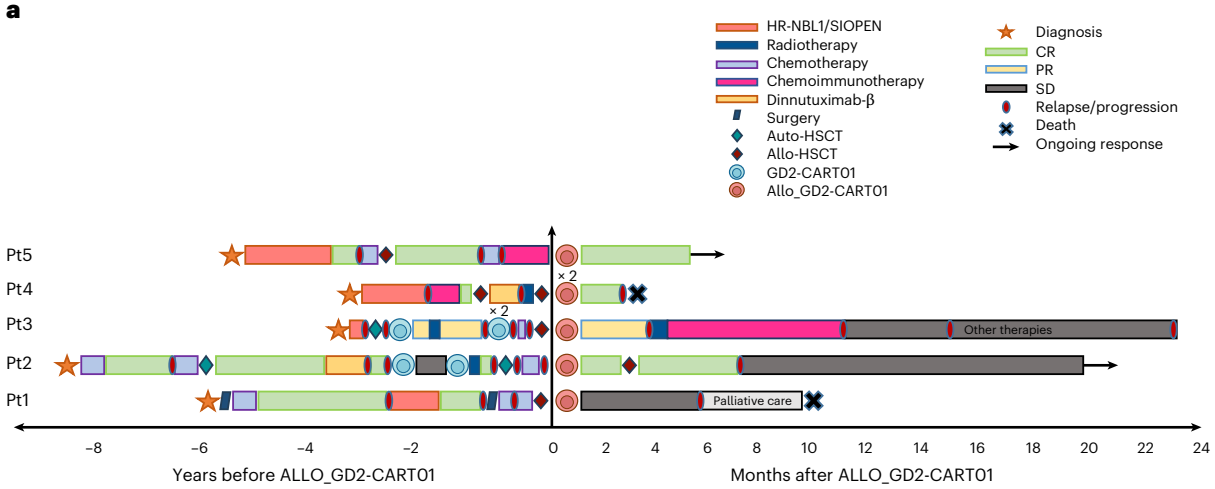

b

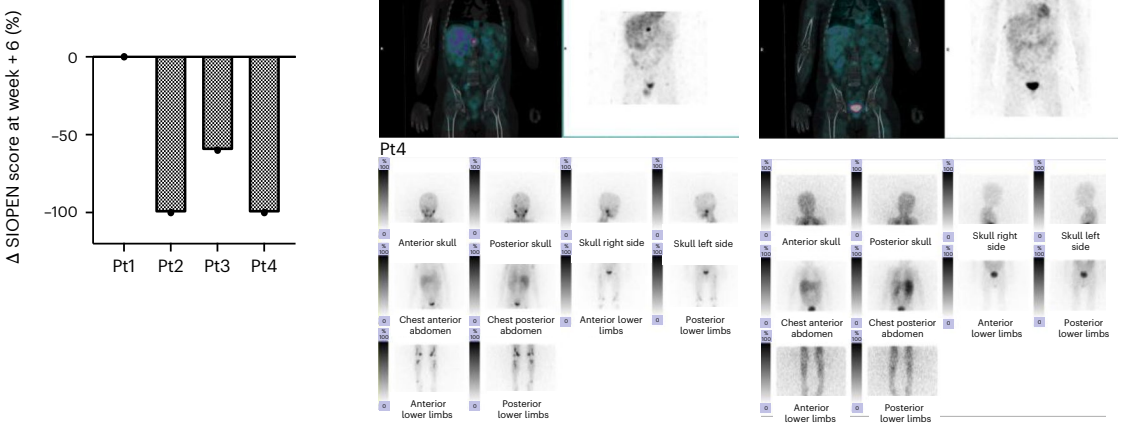

c

	Pt1	Pt2	Pt3	Pt4	Pt5
Before allogeneic HSCT	32	0[a]	6	0	NA
Before ALLO_GD2-CART01	16	5	5	37	0
After ALLO_GD2-CART01	16	0	2	0	0

d

	Pt1	Pt2	Pt3	Pt4	Pt5
CRS	Grade 2	Grade 2	Grade 3[a]	Grade 2	Grade 2
ICANS	–	–	Grade 2[a]	–	–
Hematological toxicity					
Hemoglobin	Grade 3	Grade 3	Grade 3	Grade 3	Grade 3
Granulocytes (ANC)	Grade 4	Grade 4	Grade 4	Grade 4	Grade 4
Platelets	Grade 4	Grade 4	Grade 3	Grade 4	Grade 4
aGVHD					
Skin	Stage 3[b]	Stage 3[b]	Stage 3[b]	Stage 2[b]	–
Liver	Stage 2[b]	–	–	–	–
Gut				–	–
Peripheral neuropathy	–	–	–	–	–
Other					
Paroxysmal supraventricular tachycardia	–	–	Grade 2	–	–
Aspiration pneumonia	–	–	–	Grade 4	–
Elevated AST:ALT	–	–	–	–	Grade 3

Table 1 | Characteristics of patients and HSCT

	Patient 1	Patient 2	Patient 3	Patient 4	Patient 5
Patient characteristics					
Age at Allo_CAR T cell infusion (years)	11	9	6	4	9
Sex	F	M	F	M	M
Relapsed or refractory disease	Relapsed	Relapsed	Refractory	Relapsed	Relapsed
Previous therapies	Chemotherapy (CBDCA-VP16, CADO), surgery, COJEC, BuMel+ASCT, radiotherapy, DB	Chemotherapy (CBDCA-VP16, TVD), BuMel+ASCT, ICE, TEMIRI, DB, AUTO_GD2-CART01, proton therapy, HD-[^{131}I]MIBG, topo/cyclo+venetoclax	Rapid COJEC, HD-[^{131}I]MIBG, AUTO_GD2-CART01, proton therapy, topo/cyclo+venetoclax	SIOPEN HR-01, chemo-immunotherapy, haplo-HSCT, HD-[^{131}I]MIBG	SIOPEN HR-01, TEMIRI, topo/cyclo, chemo-immunotherapy
MYCN status	Nonamplified	Nonamplified	Gain	Amplified	Nonamplified
Disease localization at CAR T infusion	Bone/bone marrow	Bone/bone marrow	Bone/bone marrow+paravertebral abdominal and parasternal	Bone/bone marrow	Bone marrow
HSCT characteristics					
Disease status at HSCT	PD—SIOPEN score: 32	CR	SD—SIOPEN score: 6+2 soft-tissue localizations	CR	CR
Conditioning regimen	[^{131}I]MIBG+L-PAM	Cym	Bu+TT+L-PAM	[^{131}I]MIBG	Bu+TT+L-PAM
Type of donor	Haploidentical (mother)	MFD (sibling)	Haploidentical (father)	Haploidentical (mother)	Haploidentical (mother)
Age of donor (years)	24	11	38	31	44
Sex	F	F	M	F	F
Graft manipulation	Alpha/beta and CD19 depletion	None	Alpha/beta and CD19 depletion	None	None
Cell dose infused					
CD34$^+$ cells×10^6 per kg	10.16	3.6	15.63	3.4	6.36
CD3$^+$ cells×10^6 per kg	8.21	43.3	24.26	169	
ab$^+$ T cells×10^6 per kg	0.08	40.47	0.08		
gd$^+$ T cells×10^6 per kg	7.36	2.8	23.99		
NK cells×10^{6}per kg	18.25	4.2	36.92		
CD20$^+$ B cells×10^6 per kg	0.006	16.6	0.07		

Bu+TT+L-PAM, busulphan, thiotepa and melphalan; BuMel, busulphan/melphalan; CADO, cyclophosphamide, doxorubicin and vincristine; CBDCA, carboplatin; Cym, cyclophosphamide; ICE, ifosfamide, carboplatin and etoposide; L-PAM, melphalan; MFD, matched familial donor; TEMIRI, temozolomide and irinotecan; topo/cyclo: topotecan/ cyclophosphamide; TVD, topotecan, vincristine and doxorubicin; VP16, etoposide.

administered, in this patient, for the prolonged, severe cytopenia developed after ALLO_GD2-CART01). A response to ALLO_GD2-CART01 was observed in four patients, including two CRs obtained in Pt2 and Pt4 (despite the massive progression observed before infusion), one CR maintained in Pt5 and one partial response (PR) in Pt3, with reduction in size of two soft-tissue lesions and >50% MIBG skeletal score reduction (Fig. 1b). In the first patient, an SD was obtained despite an extremely aggressive disease that had previously progressed under two different chemotherapy regimens and obtained PR with the allogeneic HSCT, after [^{131}I]MIBG therapy combined with melphalan. A detail of the SIOPEN (International Society of Paediatric Oncology Europe Neuroblastoma Group) score of the patients at each relevant time point of treatment is shown in Fig. 1c. In Pt4, in view of the results obtained, the favorable safety profile and very high risks characteristic of the disease, we decided to infuse a second ALLO_GD2-CART01 dose (3×10^6 CAR$^+$ cells per kg) on week 8 after the first infusion, without prior lymphodepletion considering that the patient was still cytopenic. Pt2 was treated initially with autologous drug product, the best response observed being SD, with a duration of response lasting 6 months, while, after receiving ALLO_GD2-CART01, the child finally obtained CR. Thus, the response to allogeneic CAR T cells was better than that observed with AUTO_GD2-CART01. For Pt3, the best response achieved after AUTO_GD2-CART01 was PR, with a duration of 15 months. During this period, the patient also underwent radiotherapy. After a subsequent relapse, she was given two additional infusions of AUTO_GD2-CART01, but her disease was demonstrated to be fully resistant. We then decided to proceed with the ALLO_GD2-CART01 infusion, obtaining a new PR.

Despite these results, the disease subsequently relapsed or progressed in the first four patients. In particular, Pt1 experienced a progression of disease, with the occurrence of new hepatic lesions, 6 months after treatment with ALLO_GD2-CART01. In Pt2, two new bone spots were observed 4 months after HSCT, which, however, did not progress up to the last evaluation, performed 24 months after infusion, despite the absence of any additional treatment. In Pt3, a disease progression was observed 3 months after ALLO_GD2-CART01 infusion. In Pt4, a massive dissemination of the disease in the central nervous system was observed after returning to the treatment center, 3.5 months after infusion. Pt5 still remains in continuous CR 6 months after ALLO_GD2-CART01.

https://doi.org/10.1038/s41591-024-03449-x

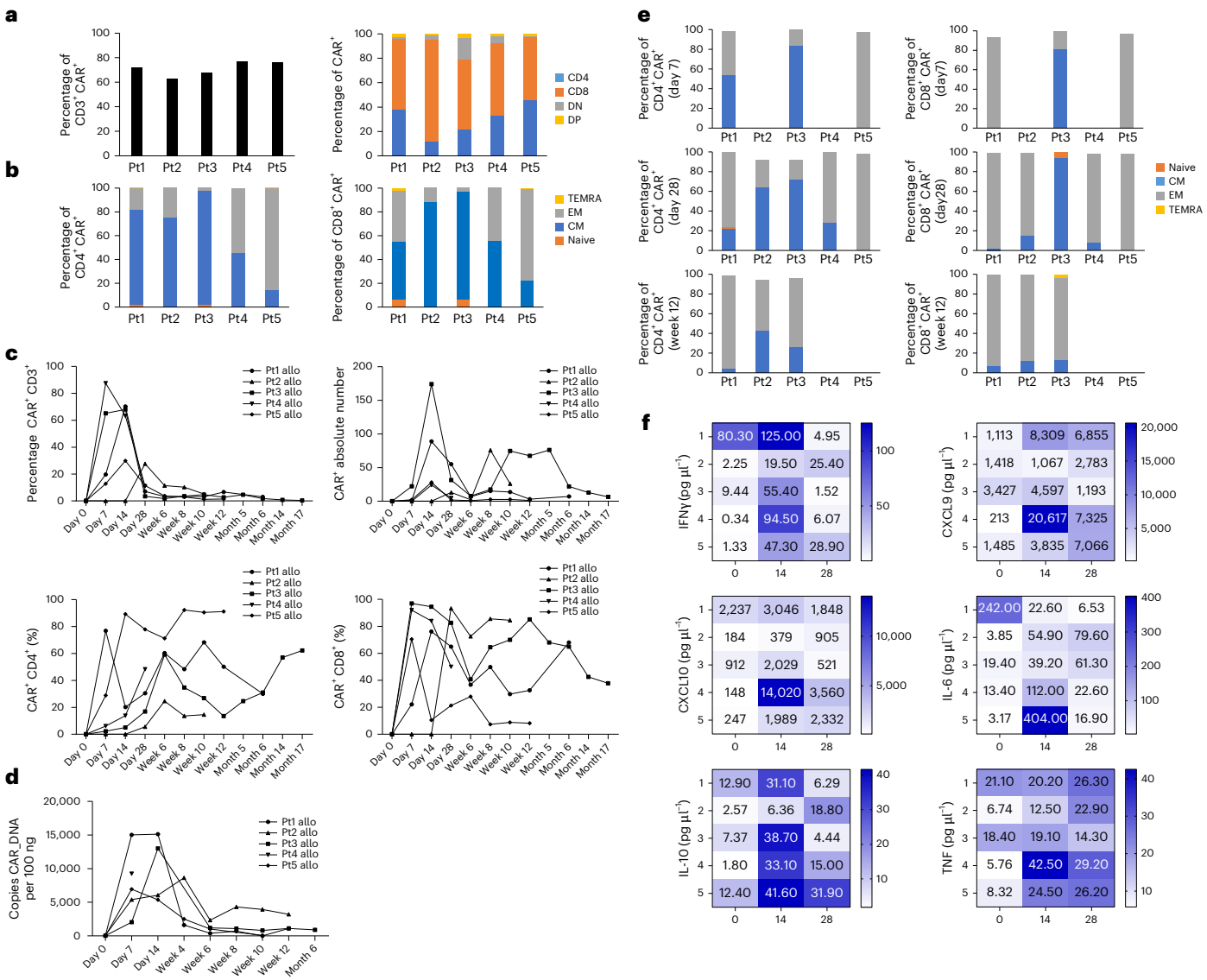

Fig. 2 | Expansion, persistence and biodistribution of ALLO_GD2-CART01. **a**,**b**, Multiparametric flow cytometry analysis of ALLO_GD2-CART01 drug product, in terms of $CD4^+CD8^+CD4^-CD8^-CD3^+$ (double negative (DN)) or $CD4^+CD8^+CD3^+$ (double positive (DP)) CAR^+ T cells (**a**), $CD4^+$ or $CD8^+$ naive ($CCR7^+/CD45RO^-$) T_{CM} cells ($CCR7^+/CD45RO^+$), T_{EM} cells ($CCR7^-/CD45RO^+$), TEMRA cells ($CCR7^-/CD45RO^-$) (**b**). **c**, Expansion and persistence of ALLO_GD2-CART01 in the PB of the patients, evaluated by flow cytometry in terms of CAR^+CD3^+ (percentage and absolute number). CAR^+CD4^+ and CAR^+CD8^+ subpopulations are shown at different time points. **d**, Expansion and persistence of ALLO_GD2-CART01 in PB of the patients, evaluated by ddPCR in terms of copies of CAR T cells per 100 ng of DNA at different time points. For Pt4, all tested samples, except for the day 7 time point, were below the acceptable threshold for low copies of the housekeeping gene and, therefore, were not included in the graph. **e**, Multiparametric flow cytometry analysis of ALLO_GD2-CART01 at day 7, day 12 and week 12 (w12) after infusion, to characterize $CD4^+$ and $CD8^+$ CAR^+ T cells for their memory profile (naive ($CCR7^+/CD45RO^-$ and $CD62L^+/CD45RA^+$), T_{CM}cells ($CCR7^+/CD45RO^+$), T_{EM} cells ($CCR7^-/CD45RO^+$) and TEMRA cells ($CCR7^-/CD45RO^-$)). The pie chart is not present when the CAR T cells were undetectable or when the number of CAR^+ T cells in each memory subset was below the threshold of 20 cells. **f**, Cytokine level in the PB of patients after ALLO_GD2-CART01 infusion at specific time points of day 0 (before infusion), day 7 and day 24 after infusion. For the specific cytokine profile of patients experiencing grade 3 CRS, refer to Extended Data Fig. 3.

Pharmacokinetics of ALLO_GD2-CART01

ALLO_GD2-CART01 expanded substantially in all patients (including Pt2, treated before allogeneic HSCT), as assessed by flow cytometry and digital droplet PCR (ddPCR; Fig. 2c,d), with high correlation between the assays (Extended Data Fig. 2a,b). In particular, we observed a CAR^+ T cell peak of 70% (89 CAR^+ T cells per µl) in Pt1, 28% (13 CAR^+ T cells per µl) in Pt2, 78% (326 CAR^+ T cells per µl) in Pt3, 72% (27 CAR^+ T cells per µl) in Pt4 and 30% (28 CAR^+ T cells per µl) in Pt5 (Fig. 2c, upper panel). It is interesting that we noticed a preferential expansion of CAR^+CD4^+ cells in Pt1 and Pt4 and a long-term predominance (>70%) of the $CD4^+$ subset for Pt5 (Fig. 2c, lower panel, left side) compared with Pt2 and Pt3 in whom a preferential expansion of CAR^+CD8^+ cells was observed (Fig. 2c, lower panel, right side). Long-term persistence (up to 6 months in all three evaluable patients, namely Pt1, Pt3 and Pt5) of ALLO_GD2-CART01 was also confirmed by ddPCR (Fig. 2d). Notably, in Pt4 the second dose also expanded, providing a second peak of circulating ALLO_GD2-CART01, despite the absence of prior lymphodepletion (Extended Data Fig. 2c,d). Although, as shown in Extended Data 3a, in Pt3 the kinetics of expansion was comparable with that observed with the autologous product, in Pt2 the CAR^+ T cell expansion reached a significantly higher magnitude and persisted remarkably longer compared with what had been observed when the same patient had been

https://doi.org/10.1038/s41591-024-03449-x

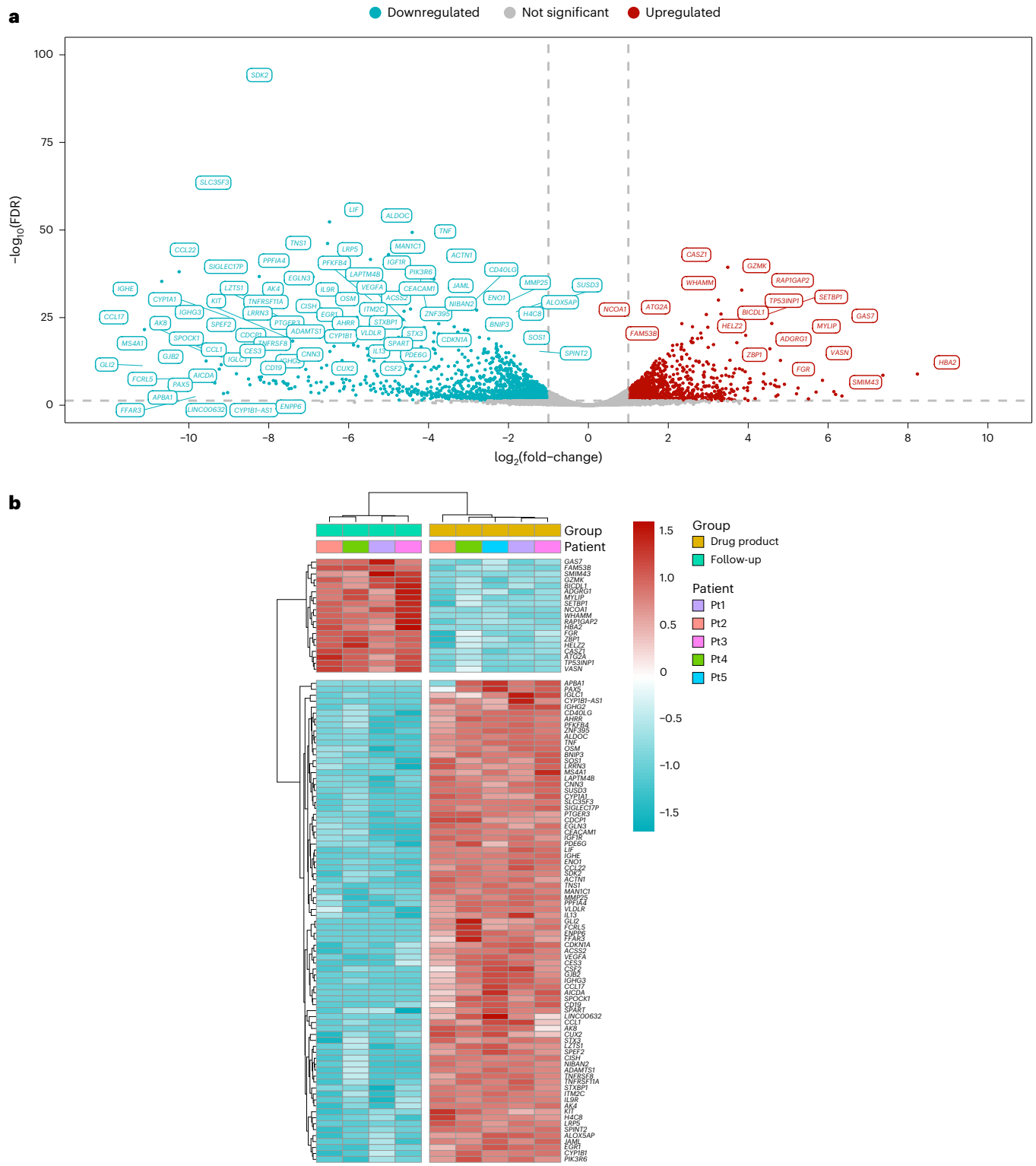

Fig. 3 | Differential gene expression profile of allogeneic GD2-CAR T cells expanded into the patient (follow-up) compared with that of the drug products. a, Volcano plot visualizing differential gene expression between GD2-CAR T cells expanded in vivo (at the peak of expansion after infusion) compared with their drug products, which were used as the baseline. The *P* values resulting from the differential gene expression analysis were assessed by a likelihood ratio test, a two-sided test, and adjusted for multiple comparisons using the Benjamini–Hochberg (BH) procedure to control for the FDR. The vertical lines correspond to the thresholds used for the $\log_2$(FC), showing upregulation ($\log_2$(FC) ≥ 1) and downregulation ($\log_2$(FC) ≤ −1). The horizontal line represents a FDR < 0.05 ($\log_{10}$ scaled). The red points on the right represent the statistically significant upregulated genes (FDR < 0.05 and $\log_2$(FC) ≥ 1) in the follow-up samples, whereas the light-blue points on the left represent upregulated genes (FDR < 0.05 and $\log_2$(FC) ≥ 1) in the drug products. The top 100 DEGs, ranked according to both FDR and $\log_2$(FC), are labeled in the plot. **b**, Heatmap of the top 100 DEGs in CAR T cells expanded in vivo (follow-ups) versus drug product samples. Expression across each gene (or row) has been scaled so that the row mean expression is 0 and the s.d. is 1 (*z*-score). The two-color gradient from light blue to red indicates for a given gene that the sample exhibits a relatively high expression (red) or a relatively low expression (blue). Lighter shades and white represent samples with an intermediate gene expression level. Samples and genes have been reordered by hierarchical clustering-based gene *z*-scores.

treated with the autologous product, suggesting that T cell features or fitness may have a remarkable impact in modulating the drug product expansion. Circulating ALLO_GD2-CART01 shows an enrichment of the CAR$^+$ central memory T cell (T_{CM} cell; average of 45 ± 42% at day 7, 37 ± 30% at day 28 and 24 ± 19 at week 12) and effector memory T cell (T_{EM} cell; average of 53 ± 41% at day 7, 59 ± 33% at day 28 and 72 ± 22 at week 12) profile in both CD4$^+$ and CD8$^+$ subpopulations (T_{CM} cells: average of 27 ± 47% at day 7, 24 ± 40% at day 28 and 11 ± 3 at week 12; T_{EM} cells average of 70 ± 44% at day 7, 74 ± 42% at day 28 and 88 ± 5 at week 12), with a predominance of the CAR$^+$ T cells belonging to the T_{EM} cell subgroup also in long-term time points of week 12 (Fig. 2e).

Safety and tolerability of ALLO_GD2-CART01 infusion

The infusion of ALLO_GD2-CART01 was associated in all patients with the toxicities commonly observed with the autologous product (Fig. 1d). In particular, hematological toxicity grade ≥3 was observed in all children, with Pt2, Pt4 and Pt5 experiencing a prolonged (>4 weeks) neutropenia. Cytokine release syndrome (CRS) occurred in all patients and was associated with the increase of serum cytokines including CXCL9 and CXCL10, the levels of which correlated with the increase in interferon (IFN)γ during patient follow-up and at the time of CAR T cell in vivo expansion (Fig. 2f). In particular, Pt1, Pt2, Pt4 and Pt5 experienced grade 2 CRS (according to Lee's criteria)[6], whereas in Pt3 grade 3 CRS, characterized by respiratory failure requiring ventilation with helmet continuous positive airway pressure and grade 2 immune effector cell-associated neurotoxicity syndrome (ICANS), characterized by clinically relevant alteration of consciousness, developed. Moreover, she concomitantly experienced grade 2 paroxysmal supraventricular tachycardia requiring pharmacological treatment. She was treated initially with tocilizumab and steroids, with improvement of the clinical picture. However, after 2 d, the respiratory and neurological status worsened and the dimerizing agent AP1903 (rimiducid), able to activate the iC9 suicide gene, was administered. After activation of the safety switch, the patient recovered quickly, with rapid reduction of the need for ventilatory support and the full restoration of normal consciousness. In parallel, a sharp decrease of circulating ALLO_GD2-CART01 was observed (with a drop from 12% to 3%, or 55.6 to 5.4 ALLO_GD2-CART01 per µl) (Extended Data Fig. 4a), as well as the decrease of IFNγ (10 versus 1.2 pg ml^{-1}, $P = 0.002$), interleukin (IL)-10 (50.5 versus 7.7 pg ml^{-1}, $P = 1.1774 \times 10^{-6}$) and IL-6 (457.1 versus 207.9 pg ml^{-1}, $P = 0.045$), but not for tumor necrosis factor (TNF) (18.1 versus 15.3 pg ml^{-1}, $P = 0.07$; Extended Data Fig. 4b). The clinical improvement allowed for a rapid tapering of the steroid therapy.

When evaluated according to the newer American Society for Transplantation and Cellular Therapy (ASTCT) Consensus Grading for Cytokine Release Syndrome and Neurologic Toxicity Associated with Immune Effector Cells[7], grade 3 CRS developed in Pt1, Pt4 and Pt5, because of hypotension requiring low doses of vasopressor and grade 4 CRS in Pt3.

After infusion of ALLO_GD2-CART01, Pt1–Pt4 experienced acute graft-versus-host disease (aGvHD) of the skin (stage 3, overall grade II according to MAGIC criteria for Pt1, Pt2 and Pt3; stage 2, overall grade I for Pt4)[8] and Pt1 also stage 2 liver aGvHD (overall grade III aGvHD). All patients with GvHD were treated with a course of steroids combined, in Pt1 and Pt2, with extracorporeal photopheresis, with rapid resolution and tapering of the steroids. Peripheral neuropathy did not occur in any of the patients. It is interesting that the second infusion in Pt4 was well tolerated, without either occurrence of CRS or worsening of hematological toxicity.

As compared with the treatment of Pt2 and Pt3 with the autologous product, we observed a higher severity of CRS when the patients received ALLO_GD2-CART01, considering CRS grading (Pt2: 0 versus 2; Pt3: 1 versus 3) and the IL-6 cytokine elevation level (Extended Data Fig. 3b), suggesting a stronger activation of the CAR T cells deriving from the allogeneic drug product.

Transcriptome profiling of ALLO_GD2-CART01

To gain further insight into the biology of ALLO_GD2-CART01, we compared the transcriptomic profiles obtained by RNA-seq analyses of five drug products with patient-matched CAR T cells collected and sorted out from PB at the time of the expansion peak (follow-up), in four of five patients (for follow-up of Pt5, the number of reads was too low to be analyzed).

Of all genes analyzed, 2,725 were differentially expressed, of which 1,204 were upregulated at follow-up. The volcano plot in Fig. 3a and the heatmap in Fig. 3b show the differentially expressed genes (DEGs) in follow-up CAR T cells compared with drug products. In particular, among the genes with the highest differential expression (for either false discovery rate (FDR) or fold-change) upregulated in the follow-up samples compared with drug products, we observed the presence of several genes associated with T cell activation and migration, including *CASZ1* (involved in T cell differentiation and development)[9], *GZMK* (produced by T_{CM} cells and T_{EM} cells; GZMKqt0o$^+$ T cells are also usually enriched in the tumor)[10], *WHAMM* and *RAP1GAP2* (involved in actin cytoskeleton organization and membrane trafficking, relevant for CAR T cell adhesion to target cells and synapse formation)[11,12], *ATG2A* and *TP53INP1* (involved in autophagy, critical for CAR T cell survival and function under stress)[13,14], *ADGRG1* and *VCAM1* (involved in cell adhesion and migration, important for CAR T cell trafficking and tumor infiltration)[14,15], *FGR* (a tyrosine kinase involved in signal transduction and immune responses, important for CAR T cell activation and signaling)[16] and *LYST* (regulates lysosomal size and function, important for CAR T cell function and cytotoxicity)[17] (Fig. 3 and Supplementary Table 1).

To gain further insights into the biological functions of the DEGs, we conducted a biological process (BP) and Kyoto Encyclopedia of Genes and Genomes (KEGG) pathway enrichment analysis for all DEGs found during follow-up in comparison with drug products (Fig. 4). As shown in the BP dot plot and network plot (Fig. 4a,b), genes involved in the response to decreased oxygen levels and humoral immune response are significantly enriched in follow-up samples, as well as key genes involved in the cytoskeleton organization and immune-synapse formation.

Furthermore, the dot plot and network plot in Fig. 4c,d show that the most enriched KEGG pathways in samples collected during follow-up are related to the chemokine signaling pathway, cytokine–cytokine receptor interaction, hematopoietic cell lineage and HIF1-signaling pathway (response to hypoxia). Correlations between key genes with increased fold-change ($\log_2$(fold-change) ($\log_2$(FC) > 3)), such as *CCL17*, *CXCL10*, *LIF*, *IL5*, *IL4* and *IL22*, highlight that the most DEGs between drug products and follow-up samples are related to chemokine stimuli. Moreover, key genes enriched in follow-up samples are not only related to cytokine (*LIF*, *TNF*, *CD40L* and *CD27*) and chemokine signaling (*IL22*, *CXCR1* and *PF4*), but also to immune cell activation and signaling (*CYBB*, *FGR*, *HCK*, *PRKCZ* and *VAV3*), inflammatory response (*S100A8* and *S100A9*) and oxidative stress (*CYBB*).

A similar analysis was also performed on drug product and follow-up samples from five patients (named Pt6–Pt10) treated with autologous GD2-CAR T cells during the same period (Extended Data Figs. 5 and 6).

The unsupervised multidimensional scaling (MDS) analysis (Fig. 5a) and hierarchical clustering (Fig. 5b) of all samples enrolled in both datasets clearly separated them into the drug product and follow-up subsets, regardless of whether they were from allogeneic or autologous GD2-CART01. Moreover, the differential gene expression analysis between allogeneic and autologous drug product or follow-up samples, respectively, revealed a high homology in gene expression, as shown in the volcano plots in Extended Data Fig. 7a,b.

Nevertheless, comparing the enriched categories resulting from the functional enrichment analysis of DEGs from follow-up samples versus drug products of patients receiving an allogeneic or autologous product, we observed 230 and 11 BPs and KEGG pathways, respectively, in common (Extended Data Fig. 8a,b), all of which were predominantly

https://doi.org/10.1038/s41591-024-03449-x

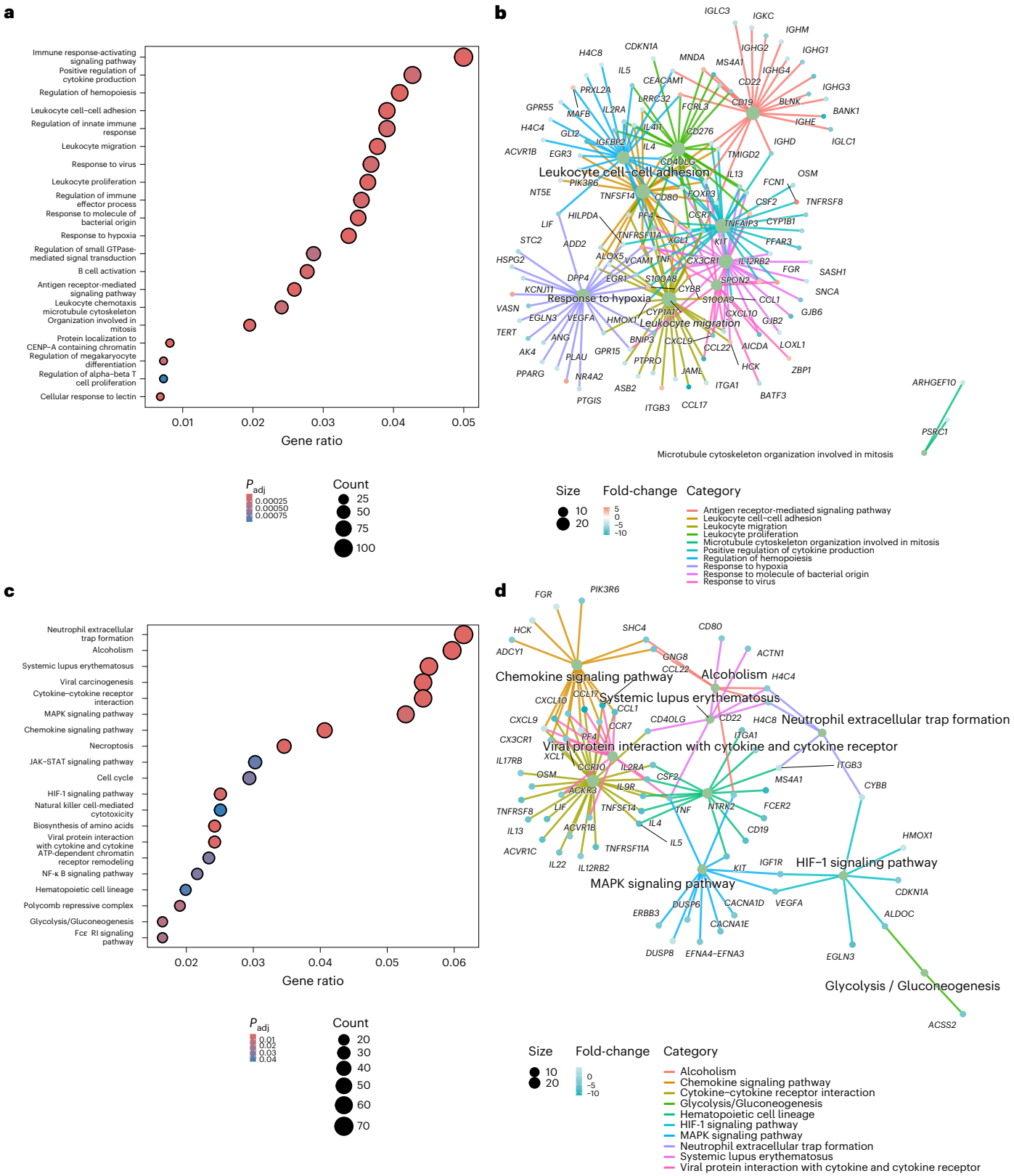

Fig. 4 | Functional enrichment analysis of DEGs in allogeneic follow-up samples. **a**,**b**, Gene ontology term enrichment analysis of DEGs found on follow-up versus drug product GD2-CAR T cell comparison, in the category of BP, shown as dot plot (**a**) and network plot (**b**). **c**,**d**, KEGG enrichment analysis of DEGs found on follow-up versus drug product GD2-CAR T cell comparison, shown as dot plot (**c**) and network plot (**d**). The enrichment analysis was conducted using the hypergeometric test, a one-sided test, to determine whether the specified term was overrepresented in the gene set of interest relative to the background. Subsequently, the *P* values were adjusted for multiple comparisons using the BH procedure to control the FDR. The plotted terms are among the top 100 BPs with $P_{adj} < 0.05$. The color and size of each dot in the dot plots represent the P_{adj} value of the term and the number of DEGs belonging to that term (gene count), respectively. The gene ratio on the *x* axis shows the proportion of the gene count as a fraction of the total number of DEGs. Networks show the interconnections between genes involved in enriched pathways. The size of the orange nodes represents the gene count of the pathway and the edge color indicates the category, as shown in the legend.

https://doi.org/10.1038/s41591-024-03449-x

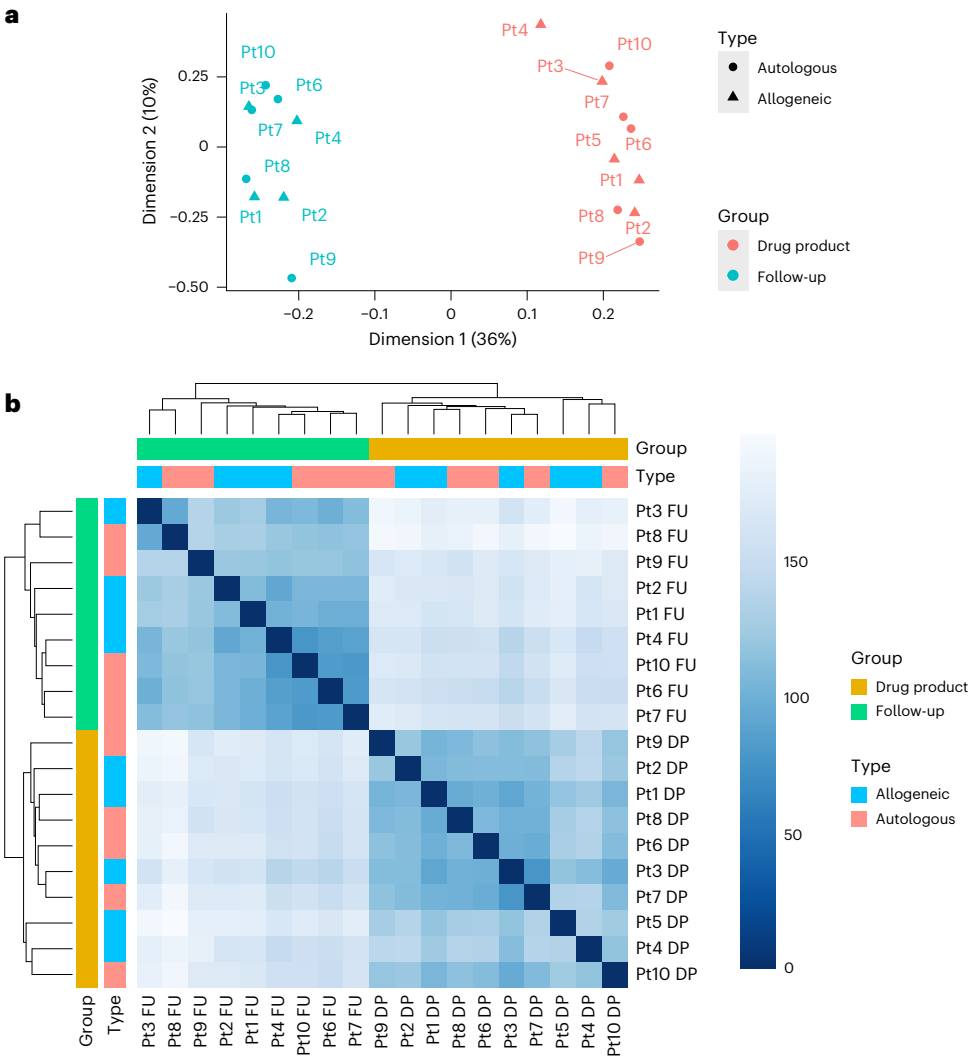

Fig. 5 | Comparison of allogeneic and autologous GD2-CAR T cells. a, Plot representing the sample positioning in the first and second dimensions of the MDS analysis. **b**, The heatmap showing the hierarchical clustering of samples based on their Euclidean distances. Regardless of the origin of the T cells (allogeneic or autologous), the samples are clearly divided into two main groups in both the analysis (drug products) and follow-ups. U, follow-up.

associated with positive regulation of T cell activation, leukocyte cell–cell adhesion, leukocyte migration, positive regulation of cytokine production and response to hypoxia. It is interesting that we also observed that 127 BP and 18 KEGG pathways characterized ALLO_GD2-CAR T cells, whereas 137 BPs and 6 KEGG pathways were predominantly associated with AUTO_GD2-CAR T cells (Extended Data Fig. 8a,b). In more detail, the allogeneic setting is characterized by pathways associated with T cell proliferation, immune synapse formation with actin filament organization and establishment of cell polarity, as well as cell chemotaxis. By contrast, in the autologous setting, many BPs were associated with the positive regulation of autophagy, glycolysis and nucleotide metabolism (Supplementary Table 2).

Discussion

Despite being obtained in a heterogeneous population of patients, the use of ALLO_GD2-CART01 was feasible and associated with both an acceptable toxicity profile and evidence of efficacy in the treatment of these multiply relapsed patients with HR-NB. ALLO_GD2-CART01 expanded robustly in all patients, reaching a peak between the second and third weeks after the infusion and persisted over time. This activation is associated with a promising antitumor effect of ALLO_GD2-CART01 cells, because three CRs (including one in a patient infused in CR) and one PR were recorded. Although the disease relapsed or progressed in three of these four patients, in Pt5 it remains in continuous CR and in Pt2 in sustained stability after relapse.

CRS was observed in every patient and was reversible in all cases, spontaneously in four of five children and with treatment, including tocilizumab, steroids and activation of the safety switch in one patient. Severe hematological toxicity developed in all patients, being attributable to lympho-depleting treatment. This toxicity profile of ALLO_GD2-CART01 cells is comparable to that observed with the autologous product[4]. Pt3 also developed ICANS requiring the activation of the iC9 suicide gene. As previously reported in the clinical trial with AUTO_GD2-CART01, the activation of the suicide gene could substantially reduce the levels of circulating GD2-CAR T cells, without resulting in a complete elimination of the engineered cells, which then re-expanded and remained persistently detectable, by both flow cytometry and ddPCR. Importantly, the toxicity resolved immediately after the administration of rimiducid, suggesting a strong efficacy also in controlling ICANS. Acute GvHD developed in four children and was rapidly controlled with a short course of therapy. Pt1 experienced liver aGvHD. Of note, at relapse, a hepatic localization of the disease was observed and we cannot exclude hepatic involvement being related to the activity of ALLO_GD2-CART01 against the liver metastasis rather than to aGvHD.

In four patients, a response was observed after infusion of ALLO_GD2-CART01, including two patients with r/r HR-NB which had previously failed to respond to the AUTO_GD2-CART01, despite the administration of lower cell doses of ALLO_GD2-CART01 than the autologous product (3×10^6 versus 10×10^6 CAR^+ T cells per kg). A CR was also achieved in Pt4, despite treatment being administered in the context of rapidly progressive disease and high disease burden and, in Pt2, treated for a highly refractory bone disease, which had previously progressed with [^{131}I]MIBG therapy and exhibited SD after chemotherapy and venetoclax. Of note, this patient was treated with ALLO_GD2-CART01 before receiving allogeneic HSCT. The gene-modified cells were not rejected and expanded remarkably, reaching a peak of 76 cells μl^{-1}. The full HLA matching with the donor, administration of lymphodepletion and the important lymphopenia at the start of treatment are all factors that probably contributed to the engraftment of ALLO_GD2-CART01 before HSCT.

Evidence from experimental animal studies, as well as clinical trials, previously demonstrated that effective allogeneic immune T cell responses can be elicited against NB[18–21]. Unfortunately, however, the graft-versus-tumor (GvT) effect was shown to be insufficient to produce a significant survival benefit in children with NB[22,23]. It is interesting that the potential of the GvT effect of allogeneic HSCT can be further harnessed by the combination with other immunotherapy approaches that actively redirect the immune system against NB cells and are effective against this tumor, including the GD2-directed monoclonal antibody and allogeneic GD2-CAR T cells. An important proof of the potential of such combinations has been recently reported by Flaadt and colleagues who showed remarkable 5-year event-free and overall survival rates of 43% and 53% in patients with r/r HR-NB receiving haploidentical HSCT with subsequent administration of dinutuximab-β to augment graft-versus-neuroblastoma effects through donor-derived natural killer cells[24].

The heterogeneity of the case series of patients whom we treated and of the HSCT received makes it difficult to generalize the results of the whole approach and to deconvolute possible synergies. However, the identification of the specific contribution of ALLO_GD2-CART01 to the outcome is possible, in each patient, thanks to: (1) the availability of a disease evaluation at each time point of treatment, that is, before HSCT and before and after ALLO_GD2-CART01 infusion; (2) the use of the same construct and manufacturing process for all the patients; and (3) the use of haploidentical donors to generate CAR T cells in all patients, except Pt2. Although the GvT effect could theoretically be long lasting after HSCT, it is difficult to consider a major contribution of the conditioning regimen and/or the GvT effect in the responses observed at later time points after allo-HSCT (all responses after ALLO_GD2-CART01 were evaluated >100 d after the infusion of the allograft and >4 months after the conditioning regimen). The observation of objective responses only 6 weeks after ALLO_GD2-CART01, coupled with the limited GvT effect and the distance from the conditioning regimen, provides important clues on the activity of ALLO_GD2-CART01.

We have proved that ALLO_GD2-CART01 may provide an attractive alternative to conventional AUTO_GD2-CART01, taking into consideration the feasibility and safety shown in each of these five patients. Beside the off-the-shelf approaches based on gene editing of the donor T cells to render them resistant to rejection and incapable of inducing GvHD, which is an appealing treatment with a different approach, donor-derived CAR T cells have raised increasing interest in the scientific community. Although no experience on solid tumors has been reported to date, in the hematological field several experiences are confirming the potential of the approach in the adult population. In particular, a promising efficacy profile without a relevant increase in toxicity has been reported across different studies[25–30]. In children, very limited experience has been published. Recently, we reported on the use of donor-derived, second-generation (4.1BB) CD19-CAR T cells in 13 children and young adults with B cell acute lymphoblastic leukemia and profound lymphopenia and/or whose disease had relapsed after allogeneic HSCT[31]. With only one case of aGvHD, controllable with immunosuppressive treatment, we observed a mild toxicity profile, coupled with 100% minimal residual disease (MRD)-negative CR in the bone marrow and CR in five of the six cases of extramedullary disease, confirming the potential of the approach[31]. These findings, although not conclusive, underline how allogeneic CAR T cells can offer an alternative curative option for patients whose disease relapses early after allogeneic HSCT or for those lacking sufficient T cell numbers to manufacture autologous CAR T cells[32].

The transcriptome profiling of allogeneic GD2-CAR T cells provides critical insights into their biological behavior and therapeutic potential. Indeed, the present study identified significant differential gene expression patterns, with 2,725 genes being differentially expressed in the samples collected from patients' PB during follow-up compared with the drug products. The upregulated genes in the follow-up samples are predominantly associated with T cell activation, migration and survival[9–17]. This suggests that in vivo CAR T cells can acquire properties useful for therapeutic efficacy. The BP and KEGG pathway enrichment analyses further elucidated the functional implications of the DEGs. The BP analysis highlighted the enrichment of genes involved in response to decreased oxygen levels, humoral immune response, cytoskeleton organization and immune-synapse formation. These processes are crucial for trafficking, infiltration and cytotoxic activity of CAR T cells within the tumor microenvironment. The KEGG pathway analysis revealed significant enrichment in pathways related to chemokine signaling, cytokine–cytokine receptor interaction, hematopoietic cell lineage and HIF1-signaling pathway, emphasizing the role of hypoxia response and chemokine stimuli in the functionality of in vivo expanded CAR T cells. Notably, key genes with high fold-changes, such as *CCL17*, *CXCL10*, *LIF*, *IL5*, *IL4* and *IL22*, indicate that chemokine signaling plays a key role in the antitumor activity of CAR T cells.

When comparing allogeneic and autologous GD2-CAR T cells, we found a high degree of homology in gene expression profiles, as evidenced by the unsupervised MDS analysis and hierarchical clustering. Both types of CAR T cells displayed similar enrichment patterns in functional categories related to T cell activation, leukocyte adhesion, migration, cytokine production and response to hypoxia. This suggests that the therapeutic mechanisms of CAR T cells, irrespective of their allogeneic or autologous origin, share common pathways essential for their antitumor activity.

However, distinct differences were observed in the DEGs between allogeneic and autologous drug products and follow-up samples. Allogeneic CAR T cells showed unique enrichment in pathways related to T cell proliferation, immune-synapse formation, actin filament organization and cell chemotaxis. These pathways are critical for the establishment of effective cell–cell interactions and sustained proliferation within the tumor microenvironment. Conversely, autologous CAR T cells were more associated with the regulation of autophagy, glycolysis and nucleotide metabolism, suggesting a more stressed profile.

The study has some limitations that must be considered in the evaluation of the results. In particular, the sample size was small, with only five patients treated. In addition, the high heterogeneity of previous treatments, very common for patients with r/r HR-NB, makes it difficult to generalize the results.

The encouraging safety profile and antitumor activity of this approach in the described case series of patients with advanced-stage disease justify further prospective investigation on ALLO_GD2-CART01 cells in a formal phase I/II clinical trial.

Online content

Any methods, additional references, Nature Portfolio reporting summaries, source data, extended data, supplementary information, acknowledgements, peer review information; details of author contributions and competing interests; and statements of data and code availability are available at https://doi.org/10.1038/s41591-024-03449-x.

References

1. Ladenstein, R. et al. Interleukin 2 with anti-GD2 antibody ch14.18/CHO (dinutuximab beta) in patients with high-risk neuroblastoma (HR-NBL1/SIOPEN): a multicentre, randomised, phase 3 trial. *Lancet Oncol.* **19**, 1617–1629 (2018).
2. Irwin, M. S. & Park, J. R. Neuroblastoma: paradigm for precision medicine. *Pediatr. Clin. North Am.* **62**, 225–256 (2015).
3. London, W. B. et al. Historical time to disease progression and progression-free survival in patients with recurrent/refractory neuroblastoma treated in the modern era on Children's Oncology Group early-phase trials. *Cancer* **123**, 4914–4923 (2017).
4. Del Bufalo, F. et al. GD2-CART01 for relapsed or refractory high-risk neuroblastoma. *N. Engl. J. Med.* **388**, 1284–1295 (2023).
5. Bai, Z. et al. Single-cell multiomics dissection of basal and antigen-specific activation states of CD19-targeted CAR T cells. *J. Immunother. Cancer* **9**, e002328 (2021).
6. Lee, D. W. et al. Current concepts in the diagnosis and management of cytokine release syndrome. *Blood* **124**, 188–195 (2014).
7. Hayden, P. J. et al. Management of adults and children receiving CAR T-cell therapy: 2021 best practice recommendations of the European Society for Blood and Marrow Transplantation (EBMT) and the Joint Accreditation Committee of ISCT and EBMT (JACIE) and the European Haematology Association (EHA). *Ann. Oncol.* **33**, 259–275 (2022).
8. Harris, A. C. et al. International, multicenter standardization of acute graft-versus-host disease clinical data collection: a report from the Mount Sinai Acute GVHD International Consortium. *Biol. Blood Marrow Transplant.* **22**, 4–10 (2016).
9. Bhaskaran, N. et al. Identification of Casz1 as a regulatory protein controlling T helper cell differentiation, inflammation, and immunity. *Front. Immunol.* **9**, 184 (2018).
10. Duquette, D. et al. Human Granzyme K Is a feature of innate T cells in blood, tissues, and tumors, responding to cytokines rather than TCR stimulation. *J. Immunol.* **211**, 633–647 (2023).
11. Piotrowski, J. T., Gomez, T. S., Schoon, R. A., Mangalam, A. K. & Billadeau, D. D. WASH knockout T cells demonstrate defective receptor trafficking, proliferation, and effector function. *Mol. Cell. Biol.* **33**, 958–973 (2013).
12. Kumar, B. V. et al. Human tissue-resident memory T cells are defined by core transcriptional and functional signatures in lymphoid and mucosal sites. *Cell Rep.* **20**, 2921–2934 (2017).
13. Valverde, D. P. et al. ATG2 transports lipids to promote autophagosome biogenesis. *J. Cell Biol.* **218**, 1787–1798 (2019).
14. Seillier, M. et al. TP53INP1, a tumor suppressor, interacts with LC3 and ATG8-family proteins through the LC3-interacting region (LIR) and promotes autophagy-dependent cell death. *Cell Death Differ.* **19**, 1525–1535 (2012).
15. Riegler, J. et al. VCAM-1 density and tumor perfusion predict T-cell infiltration and treatment response in preclinical models. *Neoplasia* **21**, 1036–1050 (2019).
16. Acin-Perez, R. et al. ROS-triggered phosphorylation of complex II by Fgr kinase regulates cellular adaptation to fuel use. *Cell Metab.* **19**, 1020–1033 (2014).
17. Turner, M. E. et al. The lysosomal trafficking regulator 'LYST': an 80-year traffic jam. *Front. Immunol.* **15**, 1404846 (2024).
18. Willems, L. et al. Recipient leukocyte infusion enhances the local and systemic graft-versus-neuroblastoma effect of allogeneic bone marrow transplantation in mice. *Cancer Immunol. Immunother.* **62**, 1733–1744 (2013).
19. Ash, S. et al. Graft versus neuroblastoma reaction is efficiently elicited by allogeneic bone marrow transplantation through cytolytic activity in the absence of GVHD. *Cancer Immunol. Immunother.* **58**, 2073–2084 (2009).
20. Inoue, M. et al. Graft-versus-tumor effect in a patient with advanced neuroblastoma who received HLA haplo-identical bone marrow transplantation. *Bone Marrow Transplant.* **32**, 103–106 (2003).
21. Willems, L., Waer, M. & Billiau, A. D. The graft-versus-neuroblastoma effect of allogeneic hematopoietic stem cell transplantation, a review of clinical and experimental evidence and a perspective on mechanisms. *Pediatr. Blood Cancer* **61**, 2151–2157 (2014).
22. Prete, A. et al. Phase II study of allogeneic hematopoietic stem cell transplantation for children with high-risk neuroblastoma using a reduced-intensity conditioning regimen: results from the AIEOP trial. *Transplant. Cell Ther.* **30**, 530 e531–530 e538 (2024).
23. Hale, G. A. et al. Allogeneic hematopoietic cell transplantation for neuroblastoma: the CIBMTR experience. *Bone Marrow Transplant.* **48**, 1056–1064 (2013).
24. Flaadt, T. et al. Anti-GD2 antibody dinutuximab beta and low-dose interleukin 2 after haploidentical stem-cell transplantation in patients with relapsed neuroblastoma: a multicenter, phase I/II trial. *J. Clin. Oncol.* **41**, 3135–3148 (2023).
25. Cruz, C. R. et al. Infusion of donor-derived CD19-redirected virus-specific T cells for B-cell malignancies relapsed after allogeneic stem cell transplant: a phase 1 study. *Blood* **122**, 2965–2973 (2013).
26. Kochenderfer, J. N. et al. Donor-derived CD19-targeted T cells cause regression of malignancy persisting after allogeneic hematopoietic stem cell transplantation. *Blood* **122**, 4129–4139 (2013).
27. Brudno, J. N. et al. Allogeneic T cells that express an anti-CD19 chimeric antigen receptor induce remissions of B-cell malignancies that progress after allogeneic hematopoietic stem-cell transplantation without causing graft-versus-host disease. *J. Clin. Oncol.* **34**, 1112–1121 (2016).
28. Chen, Y. et al. Donor-derived CD19-targeted T cell infusion induces minimal residual disease-negative remission in relapsed B-cell acute lymphoblastic leukaemia with no response to donor lymphocyte infusions after haploidentical haematopoietic stem cell transplantation. *Br. J. Haematol.* **179**, 598–605 (2017).
29. Kebriaei, P. et al. Phase I trials using Sleeping Beauty to generate CD19-specific CAR T cells. *J. Clin. Invest.* **126**, 3363–3376 (2016).
30. Locatelli, F., Del Bufalo, F. & Quintarelli, C. Allogeneic chimeric antigen receptor T cells for children with relapsed/refractory B-cell precursor acute lymphoblastic leukemia. *Haematologica* **109**, 1689–1699 (2024).
31. Del Bufalo, F. et al. Allogeneic, donor-derived, second-generation, CD19-directed CAR-T cells for the treatment of pediatric relapsed/refractory BCP-ALL. *Blood* **142**, 146–157 (2023).
32. Bader, P. Allo or auto CAR-T cells for refractory BCP-ALL? *Blood* **142**, 122–124 (2023).

https://doi.org/10.1038/s41591-024-03449-x

Concetta Quintarelli[1,2,9], Francesca Del Bufalo[1,9], Maria Antonietta De Ioris[1], Marika Guercio[1], Mattia Algeri[1,3], Daria Pagliara[1], Domenico Alessandro Silvestris[1], Matteo Di Nardo[4], Matilde Sinibaldi[1], Stefano Di Cecca[1], Laura Iaffaldano[1], Simona Manni[1], Valentina Fustaino[1], Maria Carmen Garganese[5], Giovanna Stefania Colafati[6], Valentina Bertaina[1], Marco Becilli[1], Angela Mastronuzzi[1], Francesco Fabozzi[1], Monica Gunetti[1], Stefano Iacovelli[1], Rossana Bugianesi[1], Stefania Macchia[1], Giuseppina Li Pira[1], Maria Giuseppina Cefalo[1], Giovanna Leone[7], Giada Del Baldo[1,9], Biagio De Angelis[1,9] & Franco Locatelli[1,8,9]

[1]Department of Hematology/Oncology, Cell and Gene Therapy, Scientific Institute for Research, Hospitalization and Healthcare (IRCCS), Bambino Gesù Children's Hospital, Rome, Italy. [2]Department of Clinical Medicine and Surgery, University of Naples Federico II, Naples, Italy. [3]Department of Health Sciences, Magna Graecia University, Catanzaro, Italy. [4]Pediatric Intensive Care Unit, IRCCS, Bambino Gesù Children's Hospital, Rome, Italy. [5]Nuclear Medicine Unit/Imaging Department, IRCCS, Bambino Gesù Children's Hospital, Rome, Italy. [6]Imaging Department, IRCCS, Bambino Gesù Children's Hospital, Rome, Italy. [7]Transfusion Unit, Department of Laboratories, IRCCS, Bambino Gesù Children's Hospital, Rome, Italy. [8]Catholic University of the Sacred Heart, Department of Life Sciences and Public Health, Rome, Italy. [9]These authors contributed equally: Concetta Quintarelli, Francesca Del Bufalo, Giada Del Baldo, Biagio De Angelis, Franco Locatelli. e-mail: franco.locatelli@opbg.net

Methods

Manufacture of ALLO_GD2-CART01

ALLO_GD2-CART01 was generated from lymphocytes collected from allogeneic HSC donors and transduced using a retrovirus encoding the construct iCasp9.2A.GD2.CD28.4-1BB.zeta[33]. For the manufacture of the drug products, clinical-grade viral vector has been produced by the use of 293VEC-RD114 cells (kindly provided by M. Caruso, BioVec Pharma, Inc., Canada)[4]. The manufacturing process for the production of ALLO_GD2-CART01 was identical to that used for AUTO_GD2-CART01 (ref. 4).

Patient recruitment and treatment

For each patient treated with ALLO_GD2-CART01 on the HE basis (established in the European ATMP regulation no. EC1394/2007), the approval of the research protocol and the treatment by the institutional review board and national competent authority (AIFA or Agenzia Italiana del Farmaco) was obtained before infusion on a single case basis, in accordance with current European legislation (regulation (EC) no. 1394/2007). All patient legal guardians gave written informed consent, in keeping with CARE guidelines and the Declaration of Helsinki principles.

All patients received a fludarabine/cyclophosphamide-based lymphodepletion, adjusted for the count at the moment of treatment (our conventional schema of fludarabine 25 mg m^{-2} × 3 d and cyclophosphamide 500 mg m^{-2} × 3 d for Pt2 and Pt5; a reduced schema with fludarabine 20 mg m^{-2} × 2 d and cyclophosphamide 500 mg m^{-2} × 2 d for Pt3 and only cyclophosphamide 500 mg m^{-2} × 2 d for Pt1, due to cytopenia in both; fludarabine 25 mg m^{-2} × 3 d and cyclophosphamide 1,000 mg m^{-2} × 2 d for Pt4) and a single dose of ALLO_GD2-CART01 at 3×10^6 viable CAR^+ cells per kg of recipient body weight. Only Pt4 received an additional dose of 3×10^6 viable CAR^+ cells per kg of recipient body weight, without prior lymphodepletion.

Safety and disease assessment

CRS and ICANS were evaluated according to Lee's criteria[6] and ASTCT for the newer Consensus Grading for ICANS[7].

GvHD was evaluated according to MAGIC criteria[8]. Revised International Neuroblastoma Response Criteria and SIOPEN scoring[34] were used to evaluate response.

Transgene copy number assessment by ddPCR

Primers and probes were designed complementary to the sequences coding for iC9, to detect the CAR and to the human tetratricopeptide repeat domain 5 (TTC5) for the housekeeping gene.

The following primer and probe sets were used: (1) primer/probe reaction mix (ratio 3.6) targeting the iC9 sequence of the CAR: forward primer, GCAGTGGGCTCACTCTGAAGA; reverse primer, CCCTTTCA CCGAAACAGCAT; probe, FAM-CTGCAGTCCCTCCTGCTTAGGGTCG-minor groove binder or nonfluorescent quencher; and (2) TTC5 primer or HEX-probe reaction mix (BioRad, cat. no. dHsaCP25 dHsaCP2506733), according to the BioRad protocol. Multiplex ddPCR was performed on 100 ng of DNA isolated from patients' peripheral blood mononuclear cells. The normalized CAR vector copy number was calculated by using the QX200 Droplet Digital PCR system, as follows: (iC9 vector copy numbers × number of total droplets)/TTC5 copy numbers.

Flow cytometry and immune monitoring after infusion

Flow cytometry acquisition was performed with a BD Symphony-A5 (BD Biosciences). Data analysis was performed using FACS DIVA 8.0.1 based on the gate strategy summarized in Supplementary Fig. 1. The percentage of transduced cells and detection of GD2-CART01 after infusion were determined by staining with a specific anti-idiotype antibody (1A7)[35], as previously described[33]. The following antibodies were used for phenotypic analysis of GD2-CART01: CD45, CD3, CD4, CD8, CD56, CD45Ro, CCR7, PD-1, TIM-3, TIGIT, LAG-3 and CD69 (BD Bioscience). All antibodies were used at the concentration defined by the supplier and in particular at 5 µl per test in a 100-µl final volume, with the only exception being CD8 used at 20 µl per test. Healthy donor PB was used to verify expression thresholds and gates, as well as isotype antibodies to set the fluorescence gating for each fluorochrome. Cytokine levels were analyzed in 50 samples of plasma using ELLA Elisa system (ProteinSimple/Bio-Techne) and a dedicated plate for the parallel monitoring of four cytokines, namely IL-6, IL-10, INFγ and TNF.

Bulk RNA isolation and sequencing

For the generation of RNA-seq data, we purified RNA from the clinical-grade drug products of the five patients included in the present study and their matched CAR T cells were collected from PB (follow-up) at the time of their pick (day + 16 for Pt1; day + 49 for Pt2; day + 9 for Pt3; day + 19 for Pt4; and day + 12 for Pt5). For the follow-up samples, after cell thawing, we performed sorting for the selection of CAR^+CD3^+ T cells using FACS ARIA BD. Total RNA was isolated from fresh frozen T cells using the RNeasy mini kit (QIAGEN), following the manufacturer's instructions. RNA concentration was determined with fluorometric (Qubit RNA High Sensitivity, Thermo Fisher Scientific) and electrophoretic (tape station system, Agilent) methods.

Exon libraries were constructed using the Illumina RNA Prep with Enrichment (tagmentation kit) and amplified with Exom Panel Primers (Illumina).

Briefly, 10 ng of RNA was retrotranscribed, fragmented and tagged with adaptor sequences (tagmentation, that is, tagged and fragmented) followed by purification and amplification of the purified tagmented RNA, with a target fragment size of 300–400 bp. The resulting libraries were purified with magnetic beads and target regions were captured with whole-exome oligos followed by PCR amplification of the enriched library. Exome-enriched libraries were quantified with Qbit and quality checked and sized with Tape Station system. Then, 0.8-pM paired-end libraries were amplified and ligated to the flow cell by bridge PCR and sequenced at 2× 101-bp read length, using Illumina Sequencing by synthesis technology on a NextSeq500 instrument. An average of 50 million reads for samples was obtained for transcriptomic analysis.

NextSeq500 generated bcl files for each of the four lanes. These files were converted to fastq files using Base Space.

Bioinformatics analysis

Reads that passed the trimming and filtering step of quality control were aligned by STAR v.2.7.10b to GRCh38 Ensembl genome p107. The matrix of expression was calculated using RSEM (RNA-Seq by Expectation-Maximization) v.1.3.1.

A differential expression analysis was performed using the edgeR package. The identification of DEGs was based on the application of a significant adjusted P value (P_{adj}; FDR < 0.05) and a $\log_2(FC) > 1$ (upregulated genes) or $\log_2(FC) < -1$ (downregulated genes). The overrepresentation analysis of DEGs was conducted using the clusterProfiler package[36] with the following functional databases: BP and KEGG pathway.

Statistics and reproducibility

No statistical method was used to predetermine sample size and all the patients treated have been reported. No data were excluded from the analyses. The investigators were not blinded to allocation during treatment and outcome assessment. The reported statistics were performed using GraphPad Prism 9.3.1 software.

Reporting summary

Further information on research design is available in the Nature Portfolio Reporting Summary linked to this article.

Data availability

Patient identifiable information cannot be made publicly available for reasons of patient privacy and confidentiality. However, nonidentifiable data are available from the corresponding author upon request,

based on specific criteria such as the nature of the research request and the necessary ethical approvals. The estimated time frame for responding to such requests is 2–4 weeks. Bulk RNA-seq analyzed in the present study have been uploaded to the Sequence Read Archive (SRA) at the following link: https://www.ncbi.nlm.nih.gov/sra/PRJNA1131324. All data requests will be reviewed in accordance with ethical guidelines and the sequencing data will be accessible through the SRA link at the time of publication. Source data are provided with this paper.

References

33. Quintarelli, C. et al. Choice of costimulatory domains and of cytokines determines CAR T-cell activity in neuroblastoma. *Oncoimmunology* **7**, e1433518 (2018).
34. Park, J. R. et al. Revisions to the International Neuroblastoma Response Criteria: a consensus statement from the National Cancer Institute Clinical Trials Planning Meeting. *J. Clin. Oncol.* **35**, 2580–2587 (2017).
35. Zeytin, H. E., Tripathi, P. K., Bhattacharya-Chatterjee, M., Foon, K. A. & Chatterjee, S. K. Construction and characterization of DNA vaccines encoding the single-chain variable fragment of the anti-idiotype antibody 1A7 mimicking the tumor-associated antigen disialoganglioside GD2. *Cancer Gene Ther.* **7**, 1426–1436 (2000).
36. Wu, T. et al. clusterProfiler 4.0: a universal enrichment tool for interpreting omics data. *Innovation (Camb.)* **2**, 100141 (2021).

Acknowledgements

The experimental work was supported by grants awarded by: Accelerator Award—Cancer Research UK/AIRC—INCAR project, Associazione Italiana Ricerca per la Ricerca sul Cancro (AIRC)-Special Project 5×1,000, no. 9962, AIRC IG 2018 ID 21724 (all to F.L.); AIRC IG 2023 ID 29057 (to B.D.A), MFAG 21979 (to C.Q), fellowship AIRC FIRC 'Francesco Alicino' ID25316 to M.G.; R. Corrente (to B.D.A., M.G. and S.M.), Ministero dell'Università e della Ricerca (grant nos. PRIN 2017, PRIN 2020, PRIN 2022 to F.L. and PRIN 2022 to C.Q.); Italian Health Ministry project GR-2016-02364546 (to B.D.A), RF-2016-02364388 (to F.L.), RF-2021-12374120 (to C.Q.); and the following to F.L.: European Union, Next Generation EU, Mission 4, Component 2, no. CUP B93D21010860004, National Center for Gene Therapy and Drugs Based on RNA Technology; Hub Life Science—Terapia Avanzata (LSH-TA) no. PNC-E3-2022-23683269—CUP E83C22006230001, from the Italian Health Ministry—Piano Nazionale Complementare Ecosistema Innovativo della Salute'—cod PNC-E.3, IMI JU/T2EVOLVE with grant no. 945393; and Associazione 'Raffaele Passarelli' Onlus (to B.D.A.). We thank Bio-Fab research and S. Reddel and M. Sonnessa for support with the bioinformatic analysis. We also thank M. Caruso, BioVec Pharma for the provision of 293VEC-RD114 which we used for the production of clinical-grade virus.

Author contributions

C.Q., F.D.B, B.D.A., M.A.D.I., M. Guercio, G.D.B. and F.L. designed the experimental studies, supervised the project conduction, analyzed the data and wrote the manuscript. M. Guercio, S. Manni, V.F. and D.A.S. performed RNA-seq and bioinformatics analyses. M.S., S.D.C. and L.I. performed patient immunomonitoring. V.B. performed MRD analysis on patients' bone marrow. F.D.B., M.A.D.I., G.D.B., M.A., D.P., A.M., F.F., M.B., M.G.C. and F.L. managed patients, performed data collection and interpreted clinical data. M. Gunetti, S.I., R.B. and S. Macchia were responsible for the drug product good manufacturing practice and release. G.L.P. performed apheresis manipulation. G.L. performed apheresis collection. M. Garganese revised the disease evaluation. M.D.N. managed patients in the intensive care unit. G.S.C. performed medical imaging. All authors reviewed the manuscript for final approval before submission.

Competing interests

The authors declare no competing interests.

Additional information

Extended data is available for this paper at https://doi.org/10.1038/s41591-024-03449-x.

Supplementary information The online version contains supplementary material available at https://doi.org/10.1038/s41591-024-03449-x.

Correspondence and requests for materials should be addressed to Franco Locatelli.

Peer review information *Nature Medicine* thanks Sneha Ramakrishna and the other, anonymous, reviewer(s) for their contribution to the peer review of this work. Primary Handling Editors: Saheli Sadanand and Jean Nakhle, in collaboration with the *Nature Medicine* team.

https://doi.org/10.1038/s41591-024-03449-x

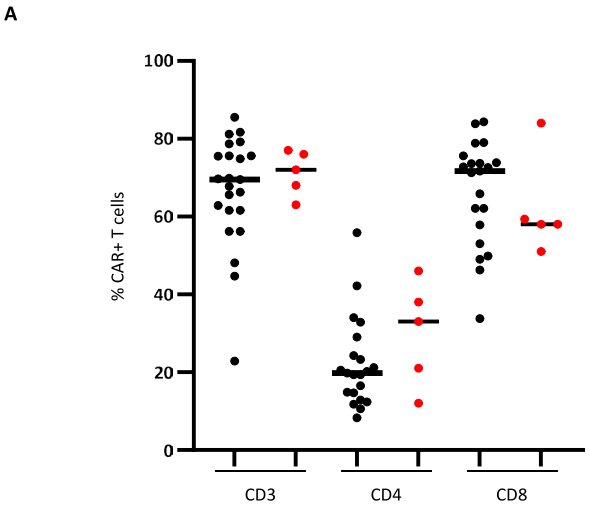

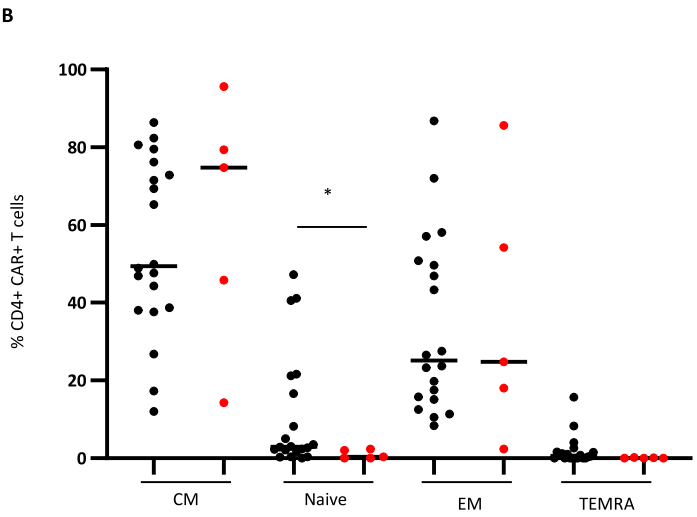

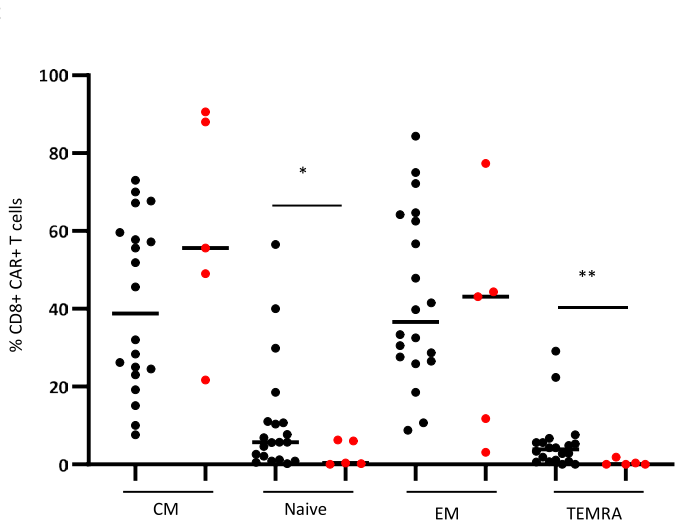

Extended Data Fig. 1 | *Characterization of allogenic and autologous* ALLO_GD2-CART01 cells in the DPs. Multiparametric flow-cytometry analysis of ALLO_GD2- CART01 (red dots) to compare the T cell composition respect to the AUTO_GD2-CART01 (black dots) of patients included in the trial (ref. 4) NCT03373097, in terms of CD4 + , CD8 + CAR + T cells (**A**), CD4+ or CD8+ Central Memory (CM), Effector Memory (EM), Terminal differentiated Effector memory (TEMRA) (**B**-**C**).

https://doi.org/10.1038/s41591-024-03449-x

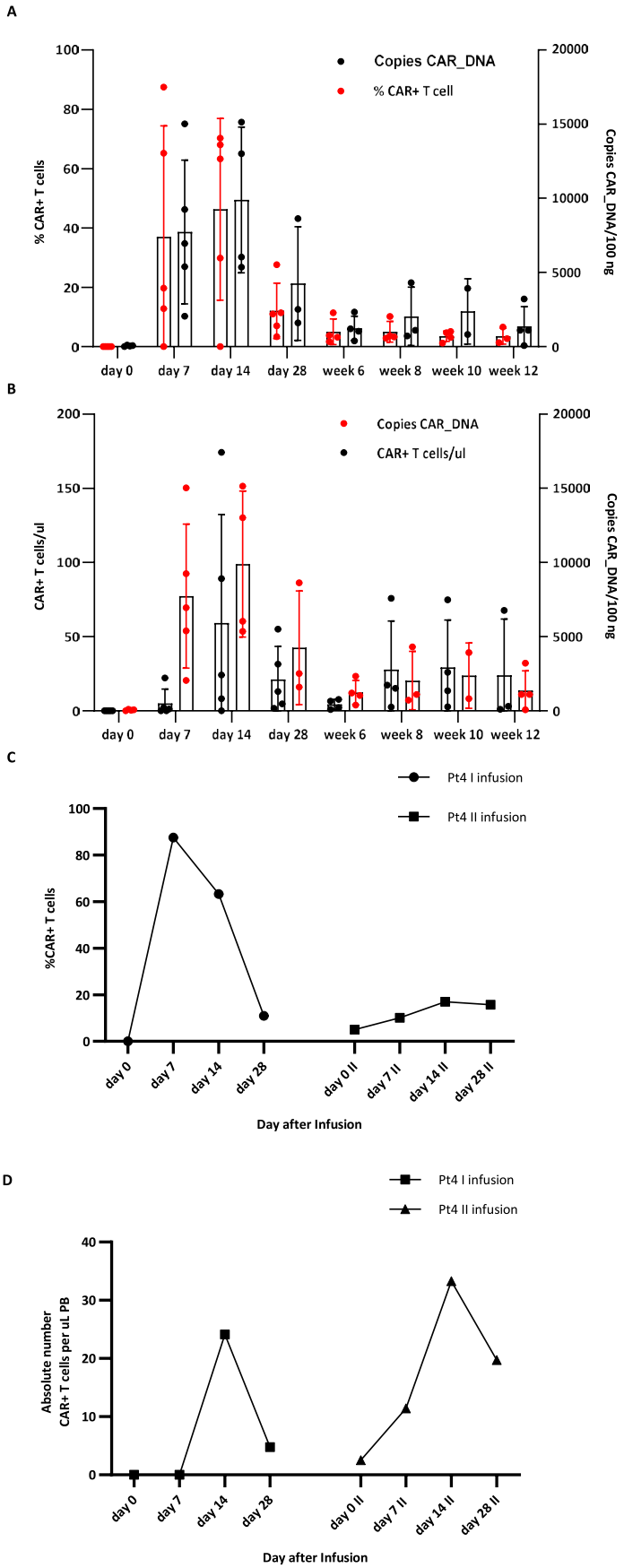

Extended Data Fig. 2 | See next page for caption.

https://doi.org/10.1038/s41591-024-03449-x

Extended Data Fig. 2 | *In vivo* expansion kinetics of ALLO_GD2-CART01 in patients after infusion. a-b Average of expansion and persistence of ALLO_GD2- CART01 in the peripheral blood of treated patients, evaluated by flow cytometry in terms of CAR^+CD3^+ (percentage (**A**) and absolute number (**B**)) vs the monitoring of genetically modified cells carried out by molecular biology (ddPCR). Data are shown as mean ± SD. **c-d** Expansion and persistence of ALLO_GD2-CART01 in Pt4's peripheral blood, evaluated by flow cytometry in terms of CAR^+CD3^+ [percentage (**C**) and absolute number (**D**)] after the first and second infusion, up to 12 weeks after the first infusion corresponding to the timeline of day 28 after the second infusion.

https://doi.org/10.1038/s41591-024-03449-x

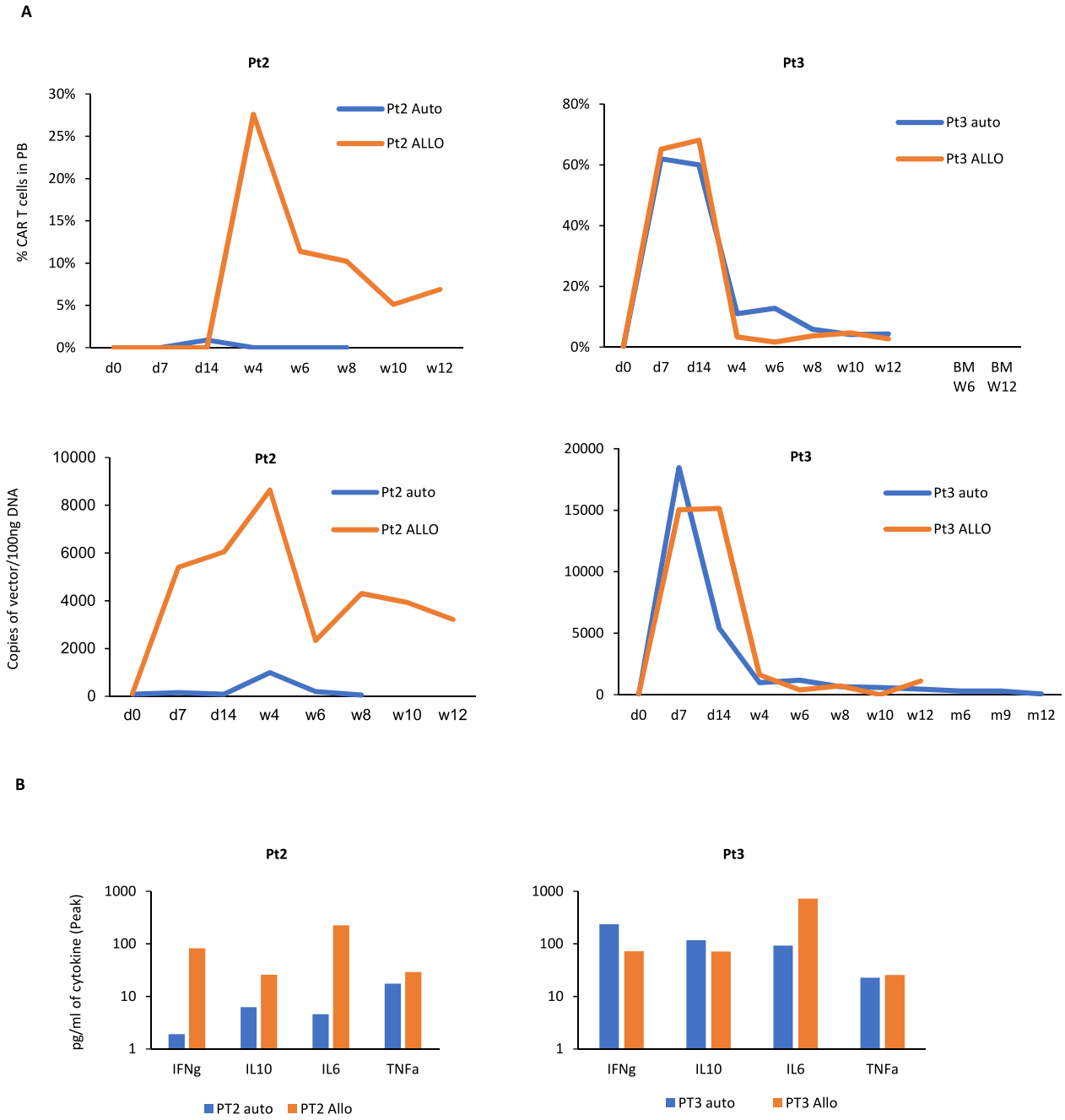

Extended Data Fig. 3 | Characterization of the kinetics of in vivo expansion of AUTO_GD2-CART01 and ALLO_GD2-CART01 in Pt2 and Pt3. (a) Kinetics of expansion and persistence of AUTO_GD2-CART01 and ALLO_GD2-CART01 after infusion in Pt2 and Pt3, evaluated by flow-cytometry (upper panels) and ddPCR (lower panels). **(b)** Cytokine levels in peripheral blood of.

https://doi.org/10.1038/s41591-024-03449-x

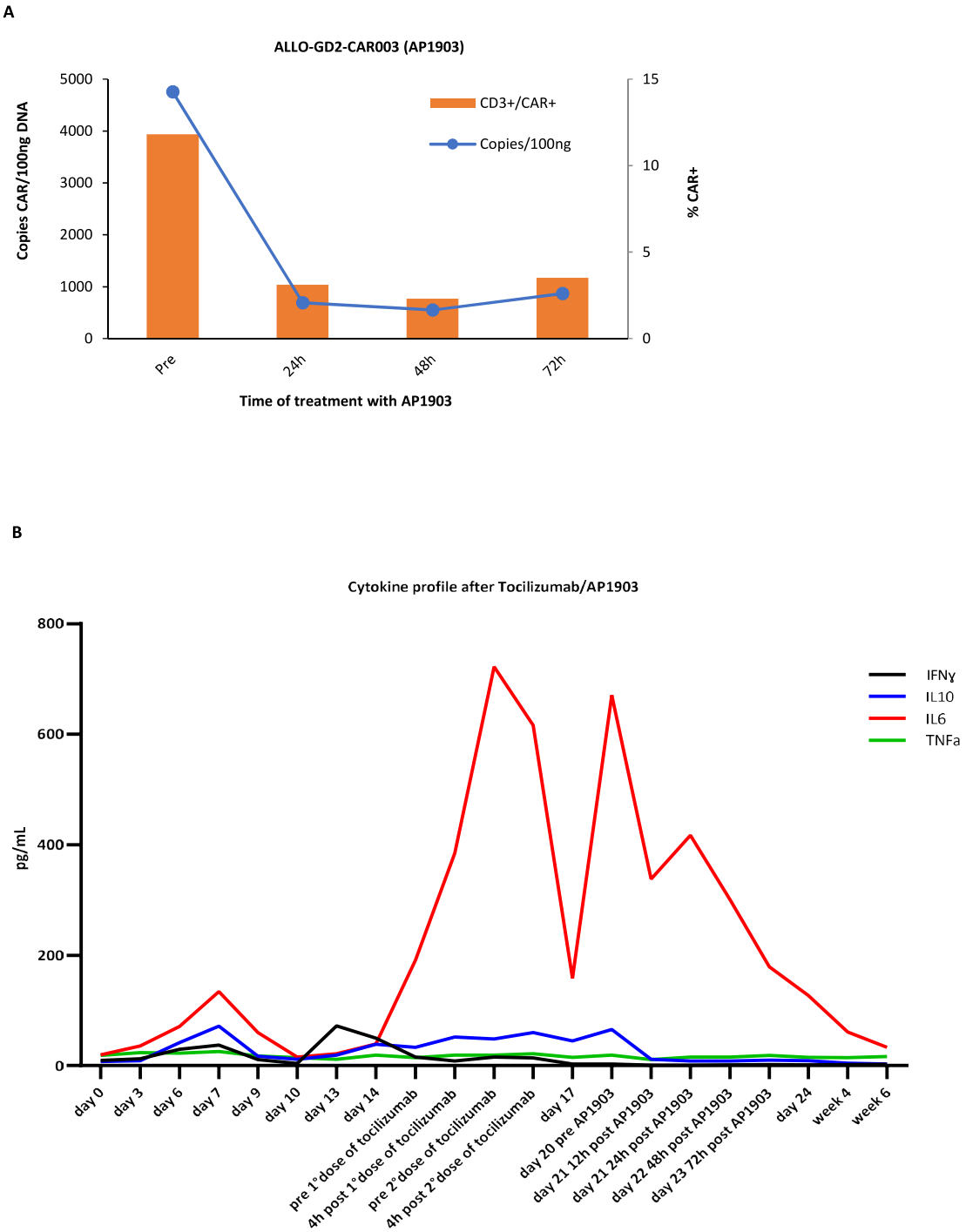

Extended Data Fig. 4 | ALLO_GD2-CART01 kinetics following the activation of the safety switch. (a) Decrease of ALLO_GD2- CART01 cells in peripheral blood of Pt3 receiving AP1903, evaluated by flow cytometry (orange columns) and ddPCR (blue line) in the first 72 hours. **(b)** Cytokine level in peripheral blood of Pt3 in the first six weeks after ALLO_GD2-CART01 infusion.

https://doi.org/10.1038/s41591-024-03449-x

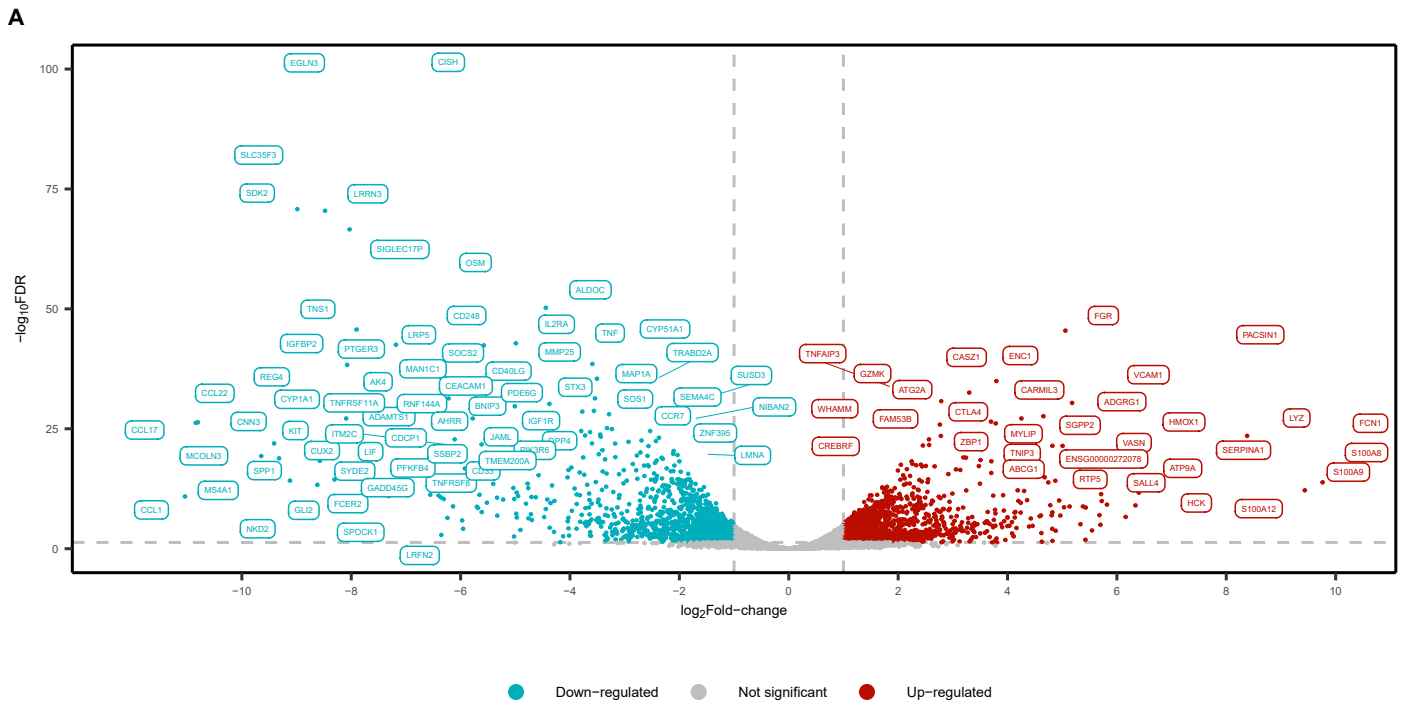

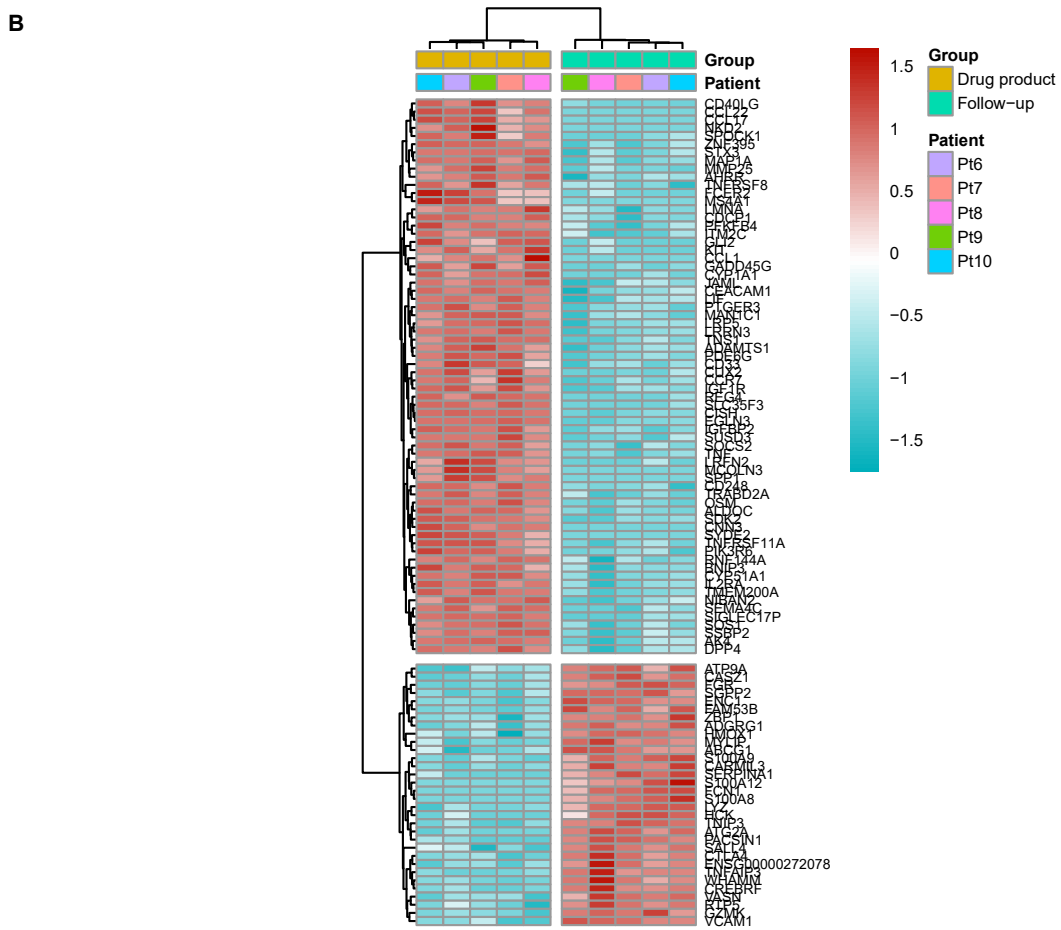

Extended Data Fig. 5 | See next page for caption.

https://doi.org/10.1038/s41591-024-03449-x

Extended Data Fig. 5 | Differential gene expression profile of autologous GD2-CAR T cells expanded into the patient (follow-ups) compared to drug products (DPs). (**a**) Volcano plot visualizing differential gene expression between GD2-CAR T cells expanded in vivo (at the peak of expansion after infusion) compared to their drug products, before infusion, which were used as the baseline. The p-values resulting from the differential gene expression analysis were assessed by a likelihood ratio test (LRT), a two-sided test, and adjusted for multiple comparisons using the Benjamini-Hochberg (BH) procedure to control for the false discovery rate (FDR). The vertical lines correspond to the thresholds used for the log2 fold-change (log2-FC), showing upregulation (log2-FC ≥ 1) and downregulation (log2-FC ≤ -1). The horizontal line represents a FDR < 0.05 (log10 scaled). The red points on the right represent the statistically significant upregulated genes (FDR < 0.05 and log2-FC ≥ 1) in the follow up (FU) samples, whilst light blue points on the left represent upregulated genes (FDR < 0.05 and log2-FC ≥ 1) in the drug products. The top 100 DEGs, ranked according to both FDR and log2-FC, are labelled in the plot. (**b**) Heat-map of the top 100 DEGs in CAR T cells expanded in vivo (FUs) vs DP samples. Expression across each gene (or row) have been scaled so that row mean expression is zero and standard deviation is one (z-score). The two-color gradient from light blue to red indicates for a given gene which sample exhibits a relatively high expression (red) or a relatively low expression (blue). Lighter shades and white represent samples with an intermediate expression level of the gene. Samples and genes have been reordered by hierarchical clustering based gene z-scores.

https://doi.org/10.1038/s41591-024-03449-x

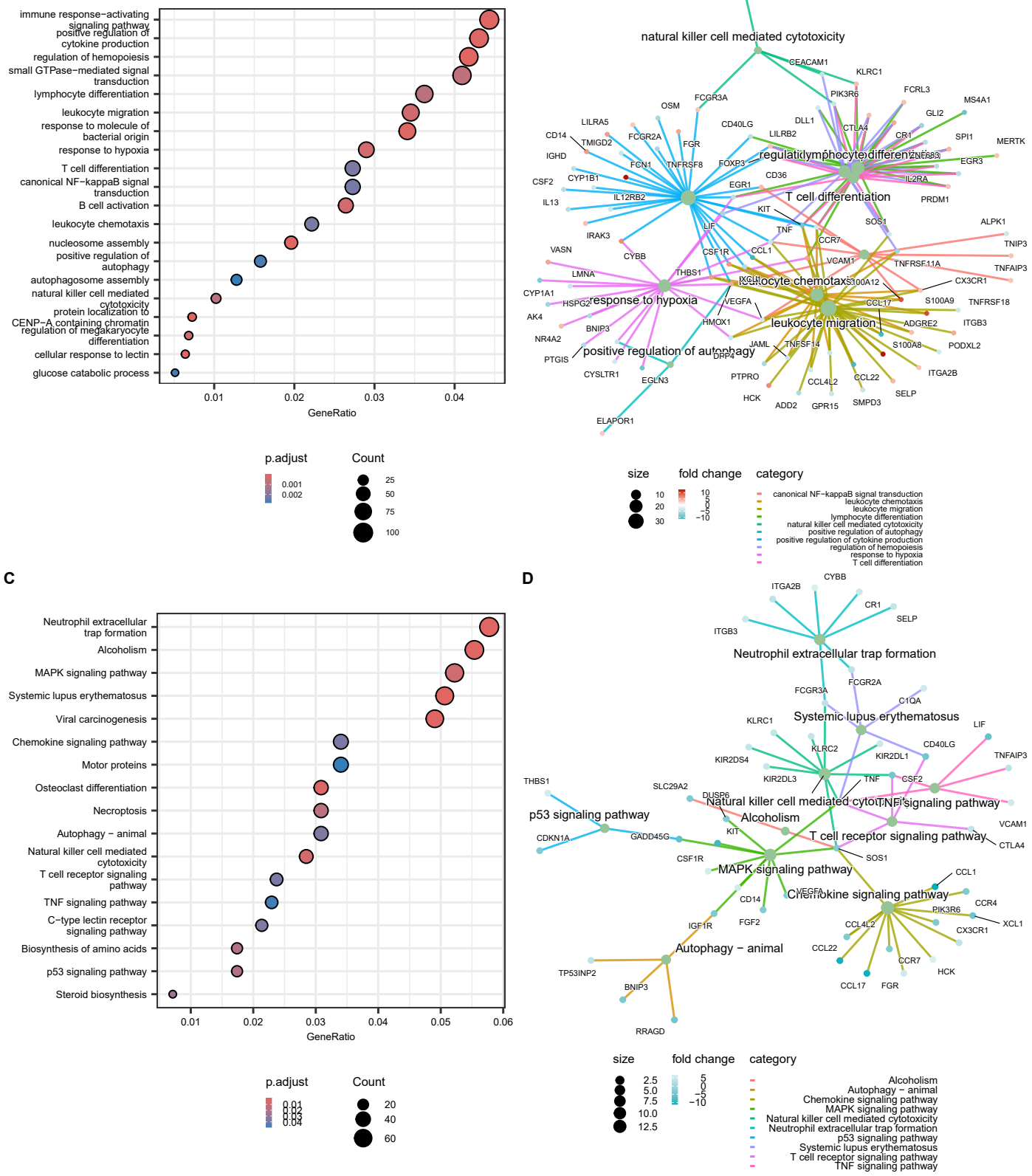

Extended Data Fig. 6 | See next page for caption.

https://doi.org/10.1038/s41591-024-03449-x

Extended Data Fig. 6 | Functional enrichment analysis of DEGs in autologous DP and follow-up samples. (**a-b**) GO terms enrichment analysis of differentially expressed genes found in follow-up versus DP GD2-CAR T cell, on the category of Biological Process. (**c-d**) KEGG enrichment analysis of differentially expressed genes found in follow-up versus DP GD2-CAR T cell comparison. The enrichment analysis was conducted using the hypergeometric test, a one-sided test, to determine whether the specified term was overrepresented in the gene set of interest relative to the background. Subsequently, the p-values were adjusted for multiple comparisons using the Benjamini-Hochberg (BH) procedure to control the false discovery rate (FDR). The plotted terms are among the top 100 BPs with an adjusted p-value of less than 0.05. The color and the size of each dot in the dot plots represents the adjusted p-value value of the term and the number of DEGs belonging to that term (gene count), respectively. The gene ratio on the x-axis shows the proportion of the gene count as a fraction of the total number of DEG. Networks show the interconnections between genes involved in enriched pathways. The size of the orange nodes represents the gene count of the pathway and the edge color indicates the category, as shown in the legend.

https://doi.org/10.1038/s41591-024-03449-x

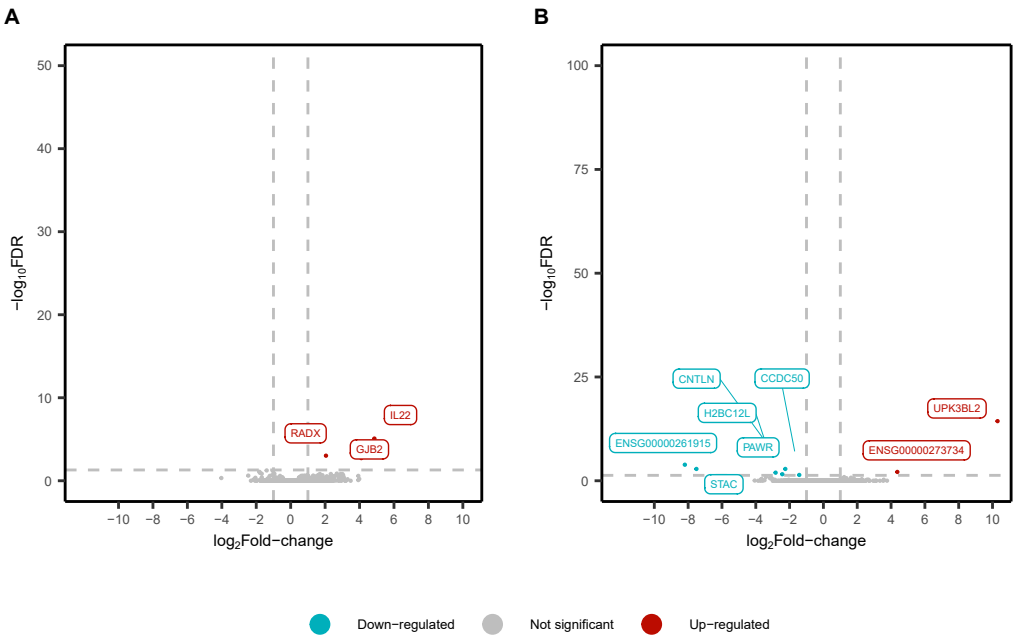

Extended Data Fig. 7 | Differential gene expression profile of allogeneic vs the baseline of autologous GD2- CAR T cells. The Volcano plots illustrate the differential gene expression between allogeneic compared to autologous drug products (**a**) and in vivo expanded (**b**) GD2-CAR T cells. The p-values resulting from the differential gene expression analysis were assessed by a likelihood ratio test (LRT), a two-sided test, and adjusted for multiple comparisons using the Benjamini-Hochberg (BH) procedure to control for the false discovery rate (FDR). The vertical lines correspond to the thresholds used for the log2 fold-change (log FC), indicating upregulation (log FC > 1) and downregulation (log FC < −1). The horizontal line represents a $P < 0.05$ (log10 scaled). The red points on the right represent the statistically significant upregulated genes ($P < 0.05$ and log FC ≥ 1) in the allogeneic samples, whilst light blue points on the left represent upregulated genes ($P < 0.05$ and log FC ≥ 1) in the autologous GD2-CAR T cells.

https://doi.org/10.1038/s41591-024-03449-x

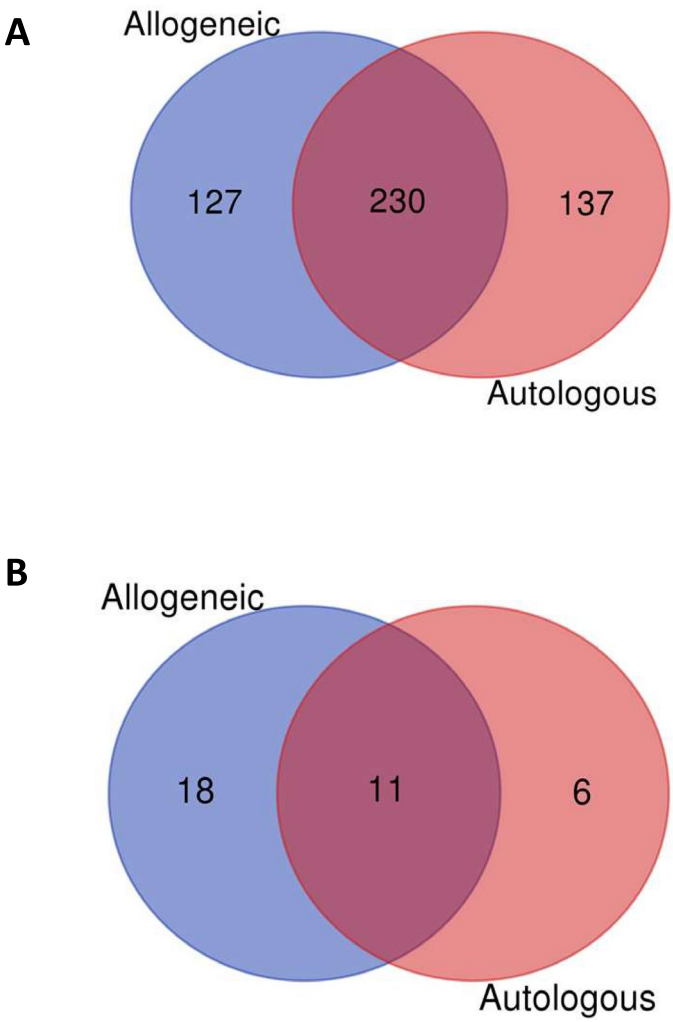

Extended Data Fig. 8 | Allogeneic vs autologous enriched categories. The Venn diagrams show the overlap between allogeneic and autologous GO biological processes (**a**) and KEGG pathways (**b**) enriched terms resulted from the functional enrichment analysis of DEGs between follow up and drug product samples.

nature portfolio

Corresponding author(s): Franco Locatelli

Last updated by author(s): Apr 12, 2024

Reporting Summary

Nature Portfolio wishes to improve the reproducibility of the work that we publish. This form provides structure for consistency and transparency in reporting. For further information on Nature Portfolio policies, see our Editorial Policies and the Editorial Policy Checklist.

Statistics

For all statistical analyses, confirm that the following items are present in the figure legend, table legend, main text, or Methods section.

n/a	Confirmed
☐	☒ The exact sample size (*n*) for each experimental group/condition, given as a discrete number and unit of measurement
☐	☒ A statement on whether measurements were taken from distinct samples or whether the same sample was measured repeatedly
☐	☒ The statistical test(s) used AND whether they are one- or two-sided *Only common tests should be described solely by name; describe more complex techniques in the Methods section.*
☒	☐ A description of all covariates tested
☒	☐ A description of any assumptions or corrections, such as tests of normality and adjustment for multiple comparisons
☐	☒ A full description of the statistical parameters including central tendency (e.g. means) or other basic estimates (e.g. regression coefficient) AND variation (e.g. standard deviation) or associated estimates of uncertainty (e.g. confidence intervals)
☐	☒ For null hypothesis testing, the test statistic (e.g. *F*, *t*, *r*) with confidence intervals, effect sizes, degrees of freedom and *P* value noted *Give P values as exact values whenever suitable.*
☒	☐ For Bayesian analysis, information on the choice of priors and Markov chain Monte Carlo settings
☒	☐ For hierarchical and complex designs, identification of the appropriate level for tests and full reporting of outcomes
☒	☐ Estimates of effect sizes (e.g. Cohen's *d*, Pearson's *r*), indicating how they were calculated

Our web collection on statistics for biologists contains articles on many of the points above.

Software and code

Policy information about availability of computer code

Data collection	RNA-Seq data were collected by on NextSeq500 instrument (Illumina). ELISA data have been mesured by ELLA Instrument by Simple Plex software (v3.9.0.28). Flow-cytometry data have been analyzed by FACSDiva software(v9.0.1). Transgene copy number was assessed by Droplet Digital™ PCR (ddPCR™, QX200 Droplet Digital PCR System, BioRad).
Data analysis	Data analysis has been performed by GraphPad Prism 9.3.1 software; RNA-Seq data were quality controlled and aligned by STAR v2.7.10b to GRCh38 Ensembl genome p107. Matrix of expression was calculate by RSEM v1.3.1. A differentially expression analysis was performed using the edgeR package. The Over-Representation Analysis (ORA) of DEGs was conducted using the clusterProfiler package.

For manuscripts utilizing custom algorithms or software that are central to the research but not yet described in published literature, software must be made available to editors and reviewers. We strongly encourage code deposition in a community repository (e.g. GitHub). See the Nature Portfolio guidelines for submitting code & software for further information.

Data

Policy information about availability of data

All manuscripts must include a data availability statement. This statement should provide the following information, where applicable:

- Accession codes, unique identifiers, or web links for publicly available datasets
- A description of any restrictions on data availability
- For clinical datasets or third party data, please ensure that the statement adheres to our policy

Patient identifiable information cannot be made publicly available for reasons of patient privacy and confidentiality. However, non-identifiable data are available from the corresponding author upon request, based on specific criteria such as the nature of the research request and the necessary ethical approvals. The estimated time frame for responding to such requests is 2-4 weeks. Bulk RNA sequencing analyzed in this study have been uploaded to Sequence Read Archive (SRA) at the following link: https://www.ncbi.nlm.nih.gov/sra/PRJNA1131324. All data requests will be reviewed in accordance with ethical guidelines, and the sequencing data will be accessible through the SRA link at the time of publication. All data generated or analysed during this study are included in this manuscript (and its supplementary information files).

Research involving human participants, their data, or biological material

Policy information about studies with human participants or human data. See also policy information about sex, gender (identity/presentation), and sexual orientation and race, ethnicity and racism.

Reporting on sex and gender	Sex and gender information was provided in the manuscript.
Reporting on race, ethnicity, or other socially relevant groupings	Reporting on race, ethnicity, or other socially grouping information was not collected because they do not affect production and effectiveness of CAR T-cells.
Population characteristics	All the relevant covariates required are described in the Table 1. Namely, all patients are affected by High Risk NB; 3 pts were male. The median age is 9 years. One patient had a MYCN amplified disease, the only relevant cytogenetic alteration of our cohort of patients.
Recruitment	Children and young adults with r/r HR-NB who had failed all potentially curative therapies (including first line treatment; chemoimmunotherapy, whenever applicable; dinutuximab-beta) but were maintaining a good performance status (Lansky/ Karnofsky score >60%), with no organ impairment, were considered for the treatment. The patients had to be ineligible for the autologous approach (either for previous failure, or for lymphopenia). Considering that the patients were treated in an hospital exemption setting, and not in a phase I/II study, no other eligibility criteria were considered and this population compares to a real world setting.
Ethics oversight	The handling of human samples was conducted in accordance with the Institutional Review Board (IRB) of Bambino Gesù Children's Hospital, IRCCS, Rome, Italy (OPBG; Ethics Committee Approval N°969/2015 prot.N°669LB, and N°1422/2017 prot.N°810). For all patients the treatment and the Research protocol were approved by both the Institutional Review Board and the National Competent Authority (AIFA, Agenzia Italiana del Farmaco)

Note that full information on the approval of the study protocol must also be provided in the manuscript.

Field-specific reporting

Please select the one below that is the best fit for your research. If you are not sure, read the appropriate sections before making your selection.

☒ Life sciences ☐ Behavioural & social sciences ☐ Ecological, evolutionary & environmental sciences

For a reference copy of the document with all sections, see nature.com/documents/nr-reporting-summary-flat.pdf

Life sciences study design

All studies must disclose on these points even when the disclosure is negative.

Sample size	No statistical method was used to predetermine sample size, all patients treated have been reported.
Data exclusions	No data were excluded from the analyses.
Replication	Replication in its traditional form is inapplicable to CAR T cell therapy because of its highly personalized, resource-intensive, and context-specific nature.
Randomization	Patients were not involved in a clinical trial and therefore randomisation was not applied. Treatments provided under hospital exemptions are typically intended for compassionate use rather than as part of a formal clinical trial, thus randomization is not applicable. The primary goal is to offer potentially life-saving therapies to patients with limited or no other treatment options, rather than to generate comparative efficacy data. Moreover, in cases like CAR T cell treatments, the therapy is customized to individual patients. Randomizing such patients, particularly when the treatment is delivered on a compassionate-use basis, contradicts the personalized nature of the intervention.

Blinding	The investigators were not blinded to allocation during treatment and outcome assessment.

Reporting for specific materials, systems and methods

We require information from authors about some types of materials, experimental systems and methods used in many studies. Here, indicate whether each material, system or method listed is relevant to your study. If you are not sure if a list item applies to your research, read the appropriate section before selecting a response.

Materials & experimental systems

n/a	Involved in the study
☐	☒ Antibodies
☒	☐ Eukaryotic cell lines
☒	☐ Palaeontology and archaeology
☒	☐ Animals and other organisms
☐	☒ Clinical data
☒	☐ Dual use research of concern
☒	☐ Plants

Methods

n/a	Involved in the study
☒	☐ ChIP-seq
☐	☒ Flow cytometry
☒	☐ MRI-based neuroimaging

Antibodies

Antibodies used	1) CD45 V500 (clone 2D1) - Cat. Num. 655873 –BD Bioscinces 2) CD14 PerCp5.5 (clone M□P9) – Cat. Num. 562692 – BD Pharmingen 3) CD19 PeCy7 (clone SJ25C1) – Cat. Num. 341113 – BD Biosciences 2) CD3 APCH7 (clone SK7) – Cat. Num. 641415 – BD Biosciences 3) CD4 BUV496 (clone SK3) – Cat. Num. 612936 – BD Horizon 4) CD8 FITC – Cat. Num. 555366 – BD Pharmingen 5) CD45RO BV421 (clone UCHL1) – Cat. Num. 562641 – BD Horizon 6) CCR7 PeCy5.5 (clone 150503) – Cat. Num. 561144 – BD Pharmingen 7) 1A7 PE (not commercial available; the antibody is derived from a hybridoma acquired from the ATCC company)
Validation	1)CD45 V500 (clone 2D1) - Cat. Num. 655873 –BD Bioscinces - Validation by the provider on human lymphocytes. Applied dilution as for provider indication: 100 µg/mL - 5uL/test 2) CD14 PerCp5.5 (clone M□P9) – Cat. Num. 562692 – BD Pharmingen - Validation by the provider on human peripheral blood monocytes. Applied dilution a for provider indication: 5uL/test 3) CD19 PeCy7 (clone SJ25C1) – Cat. Num. 341113 – BD Biosciences Validation by the provider on human peripheral blood B cells. Applied dilution as for provider indication: 25 µg/mL-5uL/test 2) CD3 APCH7 (clone SK7) – Cat. Num. 641415 – BD Biosciences Validation by the provider on human peripheral blood T cells. Applied dilution as for provider indication: 25 µg/mL-5uL/test 3) CD4 BUV496 (clone SK3) – Cat. Num. 612936 – BD Horizon. Validation by the provider on human peripheral blood leukocyte populations. Applied dilution as for provider indication: 200 µg/mL-5uL/test 4) CD8 FITC – Cat. Num. 555366 – BD Pharmingen - Validation by the provider on human peripheral blood lymphocytes. Applied dilution as for provider indication: 20uL/test 5) CD45RO BV421 (clone UCHL1) – Cat. Num. 562641 – BD Horizon. Validation by the provider on human peripheral blood lymphocytes. Applied dilution as for provider indication: 5uL/test 6) CCR7 PeCy5.5 (clone 150503) – Cat. Num. 561144 – BD Pharmingen Validation by the provider on human peripheral blood lymphocytes. Applied dilution as for provider indication: 25 µg/mL-5uL/test 7) 1A7 PE (not commercially available; the antibody is derived from a hybridoma acquired from the ATCC company)

Clinical data

Policy information about clinical studies

All manuscripts should comply with the ICMJE guidelines for publication of clinical research and a completed CONSORT checklist must be included with all submissions.

Clinical trial registration	NA
Study protocol	Allogeneic anti-GD2 Chimeric Antigen Receptor-Expressing T cells in a pediatric patient affected by r/r HR-NBL – hospital exemption protocol
Data collection	Data collection has been performed from February 2022 to June 2024
Outcomes	CRS and ICANS were evaluated according to Lee criteria and American Society for Transplantation and Cellular Therapy (ASTCT) Consensus Grading for immune-effector cell-associated neurotoxicity syndrome (ICANS) as well as the newer Consensus Grading for ICANS. Graft-versus-host-disease (GvHD) was evaluated according to MAGIC criteria. Revised International Neuroblastoma Response Criteria and SIOPEN scoring were used to evaluate response.

Plants

Seed stocks

Report on the source of all seed stocks or other plant material used. If applicable, state the seed stock centre and catalogue number. If plant specimens were collected from the field, describe the collection location, date and sampling procedures.

Novel plant genotypes

Describe the methods by which all novel plant genotypes were produced. This includes those generated by transgenic approaches, gene editing, chemical/radiation-based mutagenesis and hybridization. For transgenic lines, describe the transformation method, the number of independent lines analyzed and the generation upon which experiments were performed. For gene-edited lines, describe the editor used, the endogenous sequence targeted for editing, the targeting guide RNA sequence (if applicable) and how the editor was applied.

Authentication

Describe any authentication procedures for each seed stock used or novel genotype generated. Describe any experiments used to assess the effect of a mutation and, where applicable, how potential secondary effects (e.g. second site T-DNA insertions, mosiacism, off-target gene editing) were examined.

Flow Cytometry

Plots

Confirm that:

☒ The axis labels state the marker and fluorochrome used (e.g. CD4-FITC).

☒ The axis scales are clearly visible. Include numbers along axes only for bottom left plot of group (a 'group' is an analysis of identical markers).

☒ All plots are contour plots with outliers or pseudocolor plots.

☒ A numerical value for number of cells or percentage (with statistics) is provided.

Methodology

Sample preparation

Peripheral Blood samples underwent an erythrocyte-lysis step with BD Pharm Lyse™ for 10minutes in the dark at RT. Samples were then centrifuged (400g, 5 min, RT) and washed by adding of BSA Stain Buffer (BSA) (BD Biosciences). The cells were transferred in a 96 U-bottomed well plate and incubated with mAbs pre-mixed cocktail in BD Horizon Brilliant Stain Buffer, 30 µl/sample for 15 min at 4°C. 200µl of Stain Buffer (BSA) was added and the plate was centrifuged (200g, 5 min, RT). The samples were re-suspended in 300 µl of PBS, transferred in FACS tubes and acquired no longer than 15 minutes.
Percentage of transduced cells and detection of GD2CART01 after infusion were determined by staining with a specific anti-idiotype antibody (1A7) (Ref "Choice of costimulatory domains and of cytokines determines CAR T-cell activity in neuroblastoma". Oncoimmunology. Quintarelli C et al, 2018)
Healthy Donor peripheral blood was used to assess non-specific fluorescence, to verify expression thresholds and gates.
The flow cytometer performances were checked by using the Cytometer Setup & Tracking Module (BD Biosciences) and data reproducibility was validated using the Sphero™ Rainbow Calibration Particles -8 peaks- (BD Biosciences).

Instrument

BD FACSymphony™ A5 Cell Analyzer (BD Biosciences)

Software

FACSDiva Software v9.1 (BD Biosciences, USA)

Cell population abundance

Relevant cell populations within post-sort fractions were represented by CD3+ cells with more then 95% of purity evaluated by flow-cytometry analysis carried out on the post-sorted fraction.

Gating strategy

The gating strategy for Figure 1B, Figure 1C, Figure 2C , Figure 2E and Supplemental Figure A :
1) Singlets gating using SSC-H and SSC-A scatters
2) in the Singlet gate the lympho-monocytes populations are placed using SSC-A vs FSC-A
3) the CD14+ cells are excluded inverting the gate
4) in order to exclude the contamination of reticulocytes, the CD45+ cells are gated
5) in the CD45+ cells are plotted CD19+ and CD3+ lymphocytes
6) the CAR+ and Not-transduced cells are gated in the CD3+ total population
7) in the CAR+ gate the different subpopulations are distinguished using CD4 and CD8 parameters
8) the memory subpopulations in the CD4+ CAR+ and CD8+ CAR+ cells are characterised using CCR7 and CD45RO expression
NOTE : The hierarchy is indicated at the top of each plot

☒ Tick this box to confirm that a figure exemplifying the gating strategy is provided in the Supplementary Information.